The IRPL Model of Cosmology

Vincenzo Peluso[1*]

[1*] Via Don Bosco, 11, Genzano di Roma, 00045, Rome, Italy

July 5, 2023 .

Corresponding author(s). E-mail(s): fmsv.peluso@gmail.com;

Abstract

A new cosmological model is proposed that does not require dark energy, yet presents characteristics and trends that are almost comparable to those of the standard model. It differs from the standard model by an "extra path factor" that comes from a central hypothesis and results in an additional distance due to the gravitational radius. This additional distance causes the matter density parameter to rise from 0.5 to 1 from the big bang to the present, which gives rise to a non-zero pressure that drives the present acceleration phase of the universe's expansion. Remarkably, the halving of the density during nucleosynthesis solves the primordial lithium problem, although it introduces a deuterium problem. Finally, the resulting model solves the Hubble tension and the S_8 tension, and satisfies all the constraints derived from the most recent accurate measurements of the baryon acoustic oscillation and the angular power spectrum of the cosmic microwave background, despite having one less parameter due to the absence of dark energy. The same hypothesis explains the rotating motion of galaxies on a small scale and produces consequences that are comparable to those of the modified Newtonian dynamics (MOND) theory. However, although the proposed model respects the same principles and physics as the standard model, it needs to be reinterpreted within the framework of the more original space of light to appreciate the naturalness of the hypothesis and its profound implications.

Keywords: Cosmology: theory – distance scale – cosmological parameters – primordial nucleosynthesis – dark matter – Galaxy: kinematics and dynamics

1 Introduction

The standard Big-Bang model of cosmology provides a successful framework in which to understand the thermal history of our Universe and the growth of cosmic structure, but it is essentially incomplete. It requires very specific initial conditions. It postulates a uniform cosmological background, described by a spatially-flat, homogeneous and isotropic Robertson-Walker (RW) metric, with scale factor $a(t)$. Within this setting, it also requires an initial almost scale-invariant distribution of primordial density perturbations as seen, for example, in the cosmic microwave background (CMB) radiation, on scales far larger than the causal horizon at the time the CMB photons last scattered. To overcome the aforementioned requirements, it is necessary the introduction of the ad hoc hypothesis of inflation. Furthermore, according to the model, only few percent of the density in the Universe is provided by normal baryonic matter. The ΛCDM model requires two additional ad hoc components: a non-baryonic cold dark matter (CDM) and an even more mysterious dark energy, which makes up the rest.

The problem is that the crucial function of theories such as dark matter, dark energy and inflation —each in its own way tied to the big bang paradigm— is not to describe known empirical phenomena but rather to maintain the mathematical coherence of the framework itself while accounting for discrepant observations.
With the increase in experimental sensitivity, observational evidence for deviations from ΛCDM is, therefore, expected.

The agreement between the BBN (Big Bang Nucleosynthesis) and CMB (the angular power spectrum of Cosmological Microwave Background temperature anisotropies), since both constrain independently the cosmological parameters of the Standard model, is considered the strongest evidence in favour of the correctness of the standard model. Eg, the observed deuterium abundance (D/H) which in turn implies $\Omega_b h^2(BBN)$ in very good agreement with $\Omega_b h^2(CMB)$ deduced from the analysis of the angular power spectrum of the cosmic microwave background in the context of the standard model. Nevertheless, although, there is a good agreement between light element abundances (helium-4 and deuterium) deduced from observations and calculated in primordial nucleosynthesis, there remains a yet-unexplained discrepancy of ^7Li abundance higher by a factor of ~ 3 when calculated theoretically. Recently, even the measure of the primordial abundance of Deuterium shows signs of discrepancy with respect to the expected value, giving rise to a further Deuterium Tension [24].
On the other hand, the CMB Planck constraints are model dependent, therefore changing the cosmological scenario we can end with different conclusions, and anomalies and tensions between Planck and other cosmological probes are present well above the 3 standard deviations. These discrepancies, as time goes on, have persisted and strengthened despite several years of accurate analyses. The most famous and persisting anomalies and tensions of the CMB are:

1. the Hubble Tension (at 5σ) [29]: In recent years, new measurements of the Hubble constant, the rate of universal expansion, suggested major differences between two

independent methods of calculation which have huge implications for the validity of cosmology's current standard model at the extreme scales of the cosmos.
2. the lensing amplitude A_L internal anomaly (at more than 2σ) [1] : although the Planck lensing measurement is compatible with the theoretical expectation $A_L = 1$, the distributions of A_L inferred from the CMB power spectra alone indicate a preference for $A_L > 1$. Tension at more than 2σ level is apparent in $\Omega_c h^2$ and derived parameters, including H_0, Ω_m, and σ_8.
3. the S_8 tension with cosmic shear data (at 3.2σ) [10]: A tension on $S_8 = \sigma_8 \sqrt{\Omega_m/0.3}$ between the Planck data in the ΛCDM scenario and KiDS+VIKING-450 and DES-Y1 combined together.

Furthermore, the model, which is remarkably successful on scales larger than a few Megaparsecs, faces challenges on smaller scales. The most difficult ones are related with the rotation in the inner parts of spiral galaxies.

1.1 Premise to the presentation of the hypothesis

The Schwarzschild's metric, found by K. Schwarzschild (1916), is the solution of the Einstein equations for a gravitational field possessing central symmetry (such a field can be produced by any centrally symmetric distribution of matter). It completely determines the gravitational field in vacuum produced by any centrally-symmetric distribution of masses. The metric gives the connection between the metric of real space, or proper coordinates, and the metric of the four-dimensional space-time or Schwarzschild's coordinates, outside the gravitational radius.

The Friedmann–Lemaître–Robertson–Walker (FLRW) solution was developed independently by the named authors in the 1920s and 1930s. It too, as well as the Schwarzschild's solution, requires space to be spatially isotropic, i.e. no preferred direction. In contrast, it is obtained using a very different set of additional conditions: that space is filled with matter that is characterized by its density and pressure, but nothing else (no stress, no viscosity, etc.; a so-called "perfect fluid"); and that it is homogeneous, i.e same everywhere, but it can change as a function of time.

As a consequence, while the Schwarzschild solution is static and demonstrates the limits placed on a static spherical body before it must collapse to a black hole (the Schwarzschild limit does not apply to rapidly expanding matter), the FLRW equations describe an expanding or contracting cosmos that is uniformly filled with matter-energy.
While the Schwarzschild's coordinates are observer dependent and correspond to an "accelerated" frame, like that of an observer held at a fixed spatial point in the surrounding spacetime, the FLRW comoving coordinates (including the cosmic time) are universal and play the same roles as those of an observer falling freely under the influence of that object.

Although The FLRW metric is an exact solution of Einstein's field equations of general relativity, it doesn't derive from Einstein's field equations: it follows from the geometric properties of homogeneity and isotropy, that is from the symmetry

properties in the case of complete isotropy. In this special case of an isotropic space, the curvature properties are determined by just one constant which is the scalar curvature.
"To investigate the metric it is convenient to start from geometrical analogy, by considering the geometry of isotropic three-dimensional space as the geometry on a hypersurface known to be isotropic, in a fictitious four-dimensional space (This four-space is understood to have nothing to do with four-dimensional space-time). Such a space is a hypersphere; the three-dimensional space corresponding to this has a positive constant curvature." [21, pag 334]

It is possible to establish a spherical coordinate system, with inclination γ, on the spherical surface of Radius R_0 (R_0 is the "radius of curvature" of the Universe). Usually, these Spherical coordinates (R_0, $\gamma^{\diamond}$) are converted into cylindrical coordinates ($r^{\diamond}$, $t^{\diamond}$) which correspond to the cosmic coordinates (d_M, t). The resulting metric, that is the FLRW metric:

$$-ds^2 = -c^2dt^2 + a(t)^2\left(\frac{dr^2}{1-r^2/R_0^2} + r^2\mathrm{d}\theta^2 + r^2\sin^2\theta\mathrm{d}\phi^2\right) \tag{1}$$

or equivalently, since $r = R_0\sin\gamma$,

$$-ds^2 = -c^2dt^2 + a(t)^2R_0^2\left(\mathrm{d}\gamma^2 + \sin^2\gamma\left(\mathrm{d}\theta^2 + \sin^2\theta\mathrm{d}\phi^2\right)\right) \tag{2}$$

introduces a scale factor varying with time:

$$a(t) = \frac{\lambda_{emitted}}{\lambda_{received}} = \frac{1}{1+z} \tag{3}$$

However, since it evolves according to Einstein's field equations, the metric has an analytic solution to Einstein's field equations given by the Friedmann equations when the energy-momentum tensor is similarly assumed to be isotropic and homogeneous.

$$H^2 \equiv \left(\frac{\dot{a}}{a}\right)^2 = \frac{8\pi G}{3}\rho - \frac{kc^2}{a^2} + \frac{\Lambda c^2}{3} \tag{4}$$

$$\dot{H} + H^2 \equiv \frac{\ddot{a}}{a} = -\frac{4\pi G}{3}\left(\rho + \frac{3p}{c^2}\right) + \frac{\Lambda c^2}{3} \tag{5}$$

This metric and these equations are the basis of the standard big bang cosmological model including the current ΛCDM model.

This same metric and these same equations, as well as the entire Theory of Special (SR) and General Relativity (GTR) and Standard Model, are the basis of this work, whose fundamental achievement in the field of Cosmology is:

$$H(\gamma) = H_0\sqrt{\frac{\Omega_r}{a^4} + 2\frac{\Omega_m(\gamma)}{a^3} - \frac{\Omega_m(\gamma)}{a^2}} \tag{6a}$$

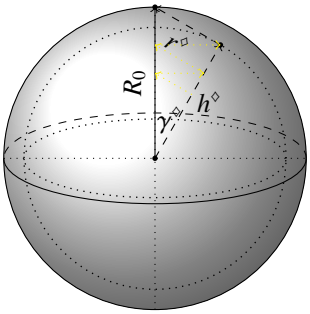

Fig. 1 hypersphere with positive curvature R_0 and universal FLRW co-moving coordinates (observer falling freely).

$$\frac{p}{c^2} = \frac{\rho_r}{3} + \frac{1}{3}\left(a - 2\,\frac{2\cos\gamma - \gamma\sin\gamma}{1 + \sin\gamma + \gamma\cos\gamma}\cos\gamma\right)\frac{\Omega_m(\gamma)}{a^3} \tag{6b}$$

where

$$\Omega_m(\gamma) = \frac{1 - \Omega_r}{(1 + \sin\gamma + \gamma\cos\gamma)^2} \quad \text{and} \quad \gamma = \arcsin\frac{z}{z+1} \tag{6c}$$

However, the (6) rests on some hypotheses that, nevertheless, are absolutely natural in the **I**ntention (or **I**nstant) **R**econstruction of **P**ath of **L**ight (IRPL) space, which is the unknown ground upon which the space-time manifold and, with it, the theories of modern physics arise. Section 2 is dedicated to the reinterpretation of current physics within the framework of this more original space of light. Then, in the following sections, the central hypothesis of the proposed model and its consequences on the cosmology are presented.

1.2 Definitions, Notation and conventions

Throughout this paper, it is indicated with:

- $R = G/c^2\, M$ the gravitational Radius
- R_Ω the constant gravitational Radius of the Universe, i.e. the constant total amount of matter-energy of the universe
- $R_{(t)} = c/H_{(t)}$ the Radius of curvature of the observable Universe, i.e. the positive curvature of the hypersphere corresponding to the observable universe
  (as usual, it is indicated with t_0 , H_0 and $R_0 = c/H_0$ respectively the cosmic time, the Hubble constant and the curvature Radius at the present time).

Finally it is assumed, on the basis of the evidence of observations, $R_\Omega = R_0 = c/H_0$.

2 The IRPL space

Light, or rather the most original wave of power which also makes light possible, builds its own realm, i.e. the physical world, through its paths in progress, whether in act or in potency, according to its own geometry. Euclidean geometry, on the contrary, was born as spatial geometry, i.e. timeless or eternal, as well as its metric consequently. In fact, it presupposes a space in which the points of a figure, for example

a triangle or a circle, are all always present together in act. This geometry is therefore not the most suitable for understanding nature in itself which, instead, is based on movement and must therefore have the path as its own unique element. Nor does it become so with the simple addition of a temporal dimension, although it acquires the ability to represent phenomena.

The double-faced sending-receiving act is the building block of the path of light. The IRPL space represents the historical reconstruction of the path of light which is enfolded and unfold from the image (the snapshot) of the world carried by the ray of light received from a sender (both from the other along the space-line and from itself along its own timeline). Each double-faced sending-receiving act unites two dual individuals, and is represented by a pair of parallel and opposite frames facing each other, composed of a common spatial axis, corresponding to the shared horizontal path of the bosons, and of the temporal axes perpendicular to it at the points where the two individuals are located. For each individual, in each point of space-time intersection (act), two shared horizontal path branch off, the incoming one of the moment of receiving and the outgoing one of the immediately following moment of giving, and therefore two temporal axes or rather two frames rotated between them by an angle γ. For each individual, the sequence of these points of intersection (points in act) composes its time axis, corresponding to the temporal path of its own baryonic matter. As light proceeds from the sender to the receiver, an individual's time axis coincides with the temporal axis of its sending frame, in the moving away, with the temporal axis of its receiving frame, in the approach.

As a result, the historical reconstruction of the series of interactions in the knowledge representation schema reveals the time axes of the individuals in the Linear pseudo-plane of Act and the plane of potency which emerges perpendicular to this. Every individual advances along its timeline by rotating in its plan of potency as a screw. The spin is preparatory to the collapse of the power wave which occurs cyclically in conjunction with the alignment of the giving-receiving spatial axis of the two subjects involved. The resulting path is made up of segments, whose quantum is the wavelength of light, which come into action only at the crossing points, in the pseudo-plane of the act, where the emission or absorption of the bosons takes place. In this scenario, the three forms of matter-energy, respectively baryonic matter, radiation and **C**old**D**ark**M**atter (CDM), correspond to the three axes of the IRPL space, respectively time, energy space and potency space.

The reciprocal rotation angle γ, as well as the mutual distance, is therefore central to the knowledge of the relationship. This knowledge may be gleaned not from a single act, because the two frames are parallelly opposed in it, but solely from the image of their wristwatches. Knowledge may thus emerge only through interactions involving entities that are complex enough to carry an image through the spatial arrangement of their components.

From a pure epistemological point of view, based on the fact that any gravitational boson has not yet been found, we can infer that while electricity is the relationship in act, fulfilled through the exchange of bosons, gravitation is the relationship only in potency, without real exchange of bosons. According to this view, gravitation is

the necessary power ground, from which matter in act is born, upon which the electric relationship can arise. That is, the blackboard is gravitational, the pencil electric. In any case, regardless of this, in the IRPL representation, despite their peculiar differences, inertial, gravitational and electric relationships follow the same universal geometric schema and can be treated in a unified way.

In the IRPL representation, the metric does not deal with abstract space and time intervals, but always and only with segments of the real path of light. Light is primitive, it is the pencil that writes on the blackboard. In other words, the space-time dualism is fictitious since light does not have a speed but, with its path, it traces the "time" and the "space" and represents the only meter (wavelength) and clock (period) on which to base the metric ($\Delta\vec{t}^{\,\diamond} = \sum \vec{r}_i^{\,\diamond}$). The plane of the Act, therefore, is a pseudo two-dimensional ($\vec{r}^{\,\diamond}$, $\vec{t}^{\,\diamond}$) linear vector space defined on the field of rational numbers (the wavelength is the quantum), where the only difference with a Euclidean vector space ($\vec{r}$, $\vec{t}$), truly two-dimensional, is that the length of the sum of the vectors is given by the algebraic sum of their lengths. In other words, the resultant of two vectors in the plane of the Act can be found using the parallelogram or triangle method, just like for Euclidean vectors but, unlike these, its length is the algebraic sum of their lengths:

$$\sin^{\diamond}\gamma + \cos^{\diamond}\gamma = 1 \qquad \text{(zero curl property)} \tag{7a}$$

$$\frac{\mathrm{d}\sin^{\diamond}\gamma}{\mathrm{d}\gamma} = -\frac{\mathrm{d}\cos^{\diamond}\gamma}{\mathrm{d}\gamma} = \cos^{\diamond}\gamma \qquad \frac{\mathrm{d}\tan^{\diamond}\gamma}{\mathrm{d}\gamma} = \frac{\mathrm{d}\,(1/\cos^{\diamond}\gamma)}{\mathrm{d}\gamma} = \frac{1}{\cos^{\diamond}\gamma} \tag{7b}$$

That is, defining in a natural way:

$$V^{\diamond} = \frac{R}{r^{\diamond}} \qquad \frac{r^{\diamond}}{\tau^{\diamond}} = \frac{p^{\diamond}}{mc} \qquad \frac{\mathbb{E}^{\diamond}}{mc^2} = \frac{t^{\diamond}}{\tau^{\diamond}} \tag{7c}$$

we have the metric:

$$\tau^{\diamond} = t^{\diamond} + r^{\diamond} \quad \text{or} \quad 1 = \frac{\mathbb{E}^{\diamond}}{mc^2} + \frac{p^{\diamond}}{mc} \tag{7d}$$

and the following two cases:

$$\frac{\mathbb{E}^{\diamond}}{mc^2} = \cos^{\diamond}\gamma \qquad \frac{p^{\diamond}}{mc} = \sin^{\diamond}\gamma \tag{7e}$$

$$\frac{\mathbb{E}^{\diamond}}{mc^2} = \frac{1}{\cos^{\diamond}\gamma} \qquad \frac{p^{\diamond}}{mc} = -\tan^{\diamond}\gamma \tag{7f}$$

representing respectively the metric of a field of forces (7e) and of an inertial system (7f).

The above equation (7a) derives clearly from a general property of the light path, that is, that the circulation along a closed path is zero (zero curl), where the sign is

positive along the direction of the light, and its demonstration rests on evidence. The remaining equations (7) derive from this or are simple definitions.

Now, the sole hypothesis of the IRPL space, necessary and sufficient to construct a general physical theory in agreement with all experiences is:

Hypothesis 1 *given that every relationship develops along the line of the present in the act of the universe in which it is enclosed, the interaction takes place in a more primitive space than space-time, which is only the External, derivative, space of Momentum. It is the original Internal space of Potential, in which the Radius and the path of the outgoing light constitute the two orthogonal axes of the potential frame of each individual. The light path connects the head of the sending Radius with the tail of the opposite receiving Radius and then crosses it (see fig. A4). In other words, unlike what happens in the external space of the momentum, in the internal space of the potential the act of sending does not immediately follow the act of reception seamless along the spatial axis but, between the two acts, the light crosses the Radius.*

It is possible to demonstrate (see A.1) that given hypothesis (1), the historical reconstruction of the light path of each cyclic interaction yields an IRPL diagram, consisting of the alternation of an external frame or Momentum and an internal one or Potential, in which:

1. the length of every segment is a multiple of the relationship wavelength $f_a(R_a) = f_b(R_b) = f_{ab}(R_a + R_b)$, that each involved individual must share, and is limited by the universe's Radius $R_0 = c/H_0$,
2. each segment develops from a geometric progression that has the energy $\mathbb{E}^\diamond$ as common ratio and a segment of a more primitive nature as scale factor, and so backwards up to the primitive elements which are the Radii of the involved individuals (see fig. A5).

Likewise, it is possible to demonstrate (see A.1) the fundamental *Principle of equivalence between inertial - not inertial systems*:

Thesis 1 *Every relationship between a sender-receiver pair, at any moment, respects the rule "Momentum" = "Potential", that is:*

$$V^\diamond = \frac{R}{r^\diamond} \quad = \quad \frac{r^\diamond}{\tau^\diamond} = \frac{p^\diamond}{mc} \tag{8}$$

where, while the momentum depends, by definition, on the Lorenz's rotation angle γ between the pair emitter-receiver, the Radius is:

$$R_p = \frac{L}{mc} = \frac{p^\diamond}{mc} r^\diamond \qquad \text{for Inertial systems (from the (8))} \tag{9}$$

$$R_m = G/c^2\, M \qquad \text{for Gravitational fields (by definition)} \tag{10}$$

Indeed, the right side of the (8) states that $\tau^\diamond$, which, from the (8), is the inverse of the acceleration $A = 1/\tau^\diamond = R/r^{\diamond 2}$, comes from a geometric progression that has $r^\diamond$ as scale factor which, in turn, based on the left side of the (8), comes from a geometric

progression that has R as scale factor (both progressions have $\mathbb{E}^\diamond/mc^2$ as common ratio). For the agreement with the experience, and how it will appear evident in the following, for Gravitational fields and inertial systems we have:

$$\sin^\diamond \gamma = \sin \gamma \tag{11}$$

Furthermore, from the zero curl property descends that the path of light of every relationship (the result of the historical reconstruction starting from the current photo) composes a geometric scheme made of an alternating succession of two dual triangle types (see fig. A3): one internal $\mathbb{G}\left(\triangle_i^\diamond\right)$, and the other external $\mathbb{G}\left(\triangle_e^\diamond\right)$ such that:

$$\mathbb{G}\left(\triangle_e^\diamond\right) = \left(\cos\gamma_e^\diamond + \sin\gamma_e^\diamond\right) = 1 \tag{12a}$$

$$\mathbb{G}\left(\triangle_i^\diamond\right) = \left(\cos\gamma_i^\diamond + \sin\gamma_i^\diamond\right) = 1 \tag{12b}$$

$$\mathbb{G}\left(\triangle_{Euclid}\right) = \mathbb{G}\left(\triangle_i^\diamond\right) \cdot \mathbb{G}\left(\triangle_e^\diamond\right) = \left(\cos\xi^2 + \sin\xi^2\right) = 1 \tag{12c}$$

where $\cos\gamma_e^\diamond = \cos\gamma^\diamond = -\cos\gamma_i^\diamond$. In particular, an internal triangle $\mathbb{G}\left(\triangle_i^\diamond\right)$ represents the potential diagram of left side of the (8), while an external triangle $\mathbb{G}\left(\triangle_e^\diamond\right)$ represents the homologue dual momentum diagram of the right side. Result the following definitions:

$$\frac{\mathbb{E}_e^\diamond}{mc^2} = \frac{\mathrm{d}t_e^\diamond}{\mathrm{d}\tau_e^\diamond} = \frac{\mathbb{E}^\diamond}{mc^2} \qquad \frac{p_e^\diamond}{mc} = \frac{\mathrm{d}r_e^\diamond}{\mathrm{d}\tau_e^\diamond} = 1 - \frac{\mathbb{E}^\diamond}{mc^2} \qquad V_e^\diamond = \frac{R}{r_e^\diamond} \tag{12d}$$

$$\frac{\mathbb{E}_i^\diamond}{mc^2} = \frac{\mathrm{d}t_i^\diamond}{\mathrm{d}\tau_i^\diamond} = -\frac{\mathbb{E}^\diamond}{mc^2} \qquad \frac{p_i^\diamond}{mc} = \frac{\mathrm{d}r_i^\diamond}{\mathrm{d}\tau_i^\diamond} = 1 + \frac{\mathbb{E}^\diamond}{mc^2} \qquad V_i^\diamond = \frac{R}{r_i^\diamond} \tag{12e}$$

The (12) make up the bridge between linear and manifold coordinates.

2.1 Linear, Minkowski, and Schwarzschild coordinate mapping

In the space-time manifold of modern physics, the element is the point, i.e. the event. This can be measured either by a frame attached to the body that generated it, or by any frame external to it. In the first case proper coordinates, i.e. wristwatch time or proper time τ and proper distance σ, are employed, which are denoted by Greek letters. All observers agree on the value of the wristwatch time or of the proper distance between two events. In the second case, however, frame coordinates r and t denoted by Latin letters are used, and these are different from frame to frame.

In the linear representation, vice versa, there are no external observers, nor does proper frame and coordinate frame dualism exist but there is only the equal relationship between two individuals within the relationship with their universal, since observer and observed are only two roles of the relationship. In the linear representation, in fact, the only measuring instruments are wristwatches synchronized at the point of contact. The number of wavelengths/periods measures space and time in a homogeneous way. The sole measurement is therefore that of the proper time, which is measured by a wristwatch attached to the transmitting body and relayed along the

path of the light to the receiver, who compares it to the time of his own wristwatch to determine the distance $r^{\diamond} = c\left(\tau^{\diamond}_{receiving} - t^{\diamond}_{sending}\right)$.

The Schwarzschild coordinates employed by GTR are substantially different from the Minkowski coordinates employed by SR, albeit, in the absence of matter, the former are reduced to the latter. The main difference derives from the fact that the SR represents the relationship through a Lorentz rotation of the two frames involved, due to each other's speed, whereas the GTR through a local deformation of the interposed space-time, due to their masses.

In the linear representation, vice versa, there are no space-time deformation, and not even a space-time in itself. The linear representation, which recognizes no other absolute outside of the relationship, leads the local deformation of the space-time predicted by the GTR to a local rotation of the two frames, according to the universal schema of fig.(A5), thus allowing a true and complete unification of the two representations.

Despite these substantial differences, the linear system is at least a legitimate system on par with the others since "the geometry of spacetime", and hence general relativity that describes it, is independent of the coordinate system used. We will show that it is also the most natural and unknowingly already used in force fields. In it, the coordinate-proper dualism is identically replaced by the send-receive dualism.

It is possible to treat inertial systems and force fields in a unified way (for the latter the relations between coordinates have a local character) considering that: about the Lorentz contraction of clocks and meters at rest at the origin

$$\frac{\tau^{\diamond}}{t^{\diamond}} = \frac{r^{\diamond}}{\sigma^{\diamond}} = \cos^{\diamond}\gamma \qquad \frac{\tau}{t} = \frac{r}{\sigma} = \frac{1}{\cosh\zeta} \text{ or } \sqrt{1-2V} \tag{13a}$$

about the metric in free fall:

$$\tau^{\diamond} = t^{\diamond} + r^{\diamond} \equiv 1 = \frac{\mathbb{E}^{\diamond}}{mc^2} + \frac{p^{\diamond}}{mc} \qquad \tau^2 = t^2 - r^2 \equiv 1 = \left(\frac{\mathbb{E}}{mc^2}\right)^2 + \left(\frac{p}{mc}\right)^2 \tag{13b}$$

with $\mathbb{E}^{\diamond} = (\cos^{\diamond}\gamma)^{\pm 1}$ where the sign of the exponent is positive for force fields, negative for inertial systems. Of course

$$\tau = \tau^{\diamond} \tag{13c}$$

About frame coordinates, let A' be the point where a signal is sent by the observer, B the arrival point on the observed body, and A the return point. In Minkowski space-time the segment $A'B$ and the segment BA are of equal length and symmetrical with respect to the spatial axis of the observer and $r = (A'B + BA)/2 = A'B(1+1)/2$ at the instant $t = (T_{A'} + T_A)/2$. In linear coordinates, on the other hand, the same measurement sees the segment $A'B$ perpendicular to the temporal axis of the observer and the segment BA ($A'B \neq BA$) perpendicular to the temporal axis of the observed rotated

by an angle γ with respect to the former. Expressed in formulas:

$$r = \frac{A'B + BA}{2} = \frac{s_2^\diamond}{2} = \frac{r^\diamond + r^\diamond \cos^\diamond \gamma}{2} = r^\diamond \left(1 - \frac{\sin^\diamond \gamma}{2}\right) \tag{13d}$$

and

$$T_A = t_A^\diamond = \tau_B^\diamond / \cos^\diamond \gamma = t_B + r = \tau_B \cosh\zeta + \tau_B \sinh\zeta \tag{13e}$$

$$T_{A'} = t_{A'}^\diamond = \tau_B^\diamond \cos^\diamond \gamma = t_B - r = \tau_B \cosh\zeta - \tau_B \sinh\zeta \tag{13f}$$

from which it follows that:

$$e^{-\zeta} \quad \equiv \quad \cos^\diamond \gamma \tag{13g}$$

The term

$$b_{\Gamma/2} = \left(1 - \frac{\sin^\diamond \gamma}{2}\right) \tag{13h}$$

in the (13d) is the conversion factor between linear and Minkowski coordinates. At last, from the (8) and the (13) we have:

$$r = \frac{s_2^\diamond}{2} = b_{\Gamma/2} r^\diamond = r^\diamond + \frac{R_p/2}{\mathbb{E}^\diamond/mc^2} = \frac{r^\diamond}{\mathbb{E}^\diamond/mc^2} - \frac{R_p/2}{\mathbb{E}^\diamond/mc^2} \tag{13i}$$

$$t = \frac{\mathbb{E}}{\mathbb{E}^\diamond} t^\diamond = \frac{\tau^\diamond}{\mathbb{E}^\diamond/mc^2} - r = \tau^\diamond(\mathbb{E}^\diamond/mc^2) + r \tag{13j}$$

2.1.1 Inertial system ($\mathrm{d}R_p \neq 0$)

When $\mathrm{d}\zeta = \mathrm{d}\gamma = 0$, that is in an inertial system, where $v = \tanh\zeta = constant$ and analogously $V^\diamond = constant$, we can follow the trend of the coordinates: $\mathrm{d}r/\mathrm{d}\tau$, $\mathrm{d}t/\mathrm{d}\tau$, as the time changes. Since

$$\frac{\mathbb{E}^\diamond}{mc^2} = \frac{1}{\cos^\diamond \gamma} \qquad p^\diamond/mc = -\tan^\diamond \gamma \qquad \frac{\mathbb{E}}{mc^2} = \frac{1}{(\cosh\zeta)^{-1}} \qquad p/mc = \pm i \sinh\zeta \tag{14a}$$

and therefore the momentum Radius R_p and spatial distance $r^\diamond$:

$$r^\diamond = -\tan^\diamond \gamma\, \tau^\diamond \qquad\qquad R_p = V^\diamond r^\diamond = -\tan^\diamond \gamma \cdot r^\diamond \tag{14b}$$

At last, from the (13i) and (13j) we have

$$v/c = \tanh\zeta = \frac{\mathrm{d}r_{Mink.}}{\mathrm{d}t_{Mink.}} = \frac{\left(r^\diamond - 1/2\, R_p\right)/\mathbb{E}^\diamond}{\tau^\diamond/\mathbb{E}^\diamond - \left(r^\diamond - 1/2\, R_p\right)/\mathbb{E}^\diamond} = \frac{1 - (1 - \sin\gamma)^2}{1 + (1 - \sin\gamma)^2} \tag{14c}$$

One of the most remarkable properties of an inertial system is:

$$\frac{\mathrm{d}r^{\diamond}}{\mathrm{d}r} \neq \frac{\mathrm{d}t^{\diamond}}{\mathrm{d}t} \qquad \left(\frac{1}{b_{\Gamma/2}} \neq \frac{\mathbb{E}^{\diamond}}{\mathbb{E}}\right) \tag{14d}$$

nevertheless, it is possible to convert the linear metric into the corresponding quadratic form considering that:

$$b_{\Gamma/2}\frac{\mathrm{d}r^{\diamond}}{\mathrm{d}r} = b_{\Gamma/2}\frac{p^{\diamond}}{p} = 1 \tag{14e}$$

and therefore

$$\frac{\mathbb{E}}{mc^2} = \sqrt{1 + b_{\Gamma/2}^2 (p^{\diamond}/mc)^2} = \frac{\mathbb{E}^{\diamond}}{mc^2} mc^2 \sqrt{\frac{1}{\mathbb{E}^{\diamond 2}} + b_{\Gamma/2}^2 \frac{(p^{\diamond}/mc)^2}{\mathbb{E}^{\diamond 2}}} = \frac{\mathbb{E}^{\diamond}}{mc^2}\frac{E}{mc^2} \tag{14f}$$

where $E/mc^2 = \mathbb{E}/\mathbb{E}^{\diamond}$. The (14f) can be re-expressed as:

$$\frac{mc^2}{\mathbb{E}} = \frac{\frac{1}{\mathbb{E}^{\diamond}}}{\sqrt{\frac{1}{\mathbb{E}^{\diamond 2}} + b_{\Gamma/2}^2 \frac{p^{\diamond 2}/m^2c^2}{\mathbb{E}^{\diamond 2}}}} \qquad \sqrt{1 - \left(\frac{mc^2}{\mathbb{E}}\right)^2} = \frac{b_{\Gamma/2}\frac{p^{\diamond}/mc}{\mathbb{E}^{\diamond}}}{\sqrt{\frac{1}{\mathbb{E}^{\diamond 2}} + b_{\Gamma/2}^2 \frac{p^{\diamond 2}/m^2c^2}{\mathbb{E}^{\diamond 2}}}} \tag{14g}$$

that is:

$$\frac{1}{\cosh\zeta} = \frac{\cos^{\diamond}\gamma}{\sqrt{\cos^{\diamond 2}\gamma + b_{\Gamma/2}^2 \sin^2\gamma}} \qquad \tanh\zeta = \frac{b_{\Gamma/2}\sin^{\diamond}\gamma}{\sqrt{\cos^{\diamond 2}\gamma + b_{\Gamma/2}^2 \sin^2\gamma}} \tag{14h}$$

Since $\mathrm{d}\tau^{\diamond}/\mathrm{d}t^{\diamond} = \mathbb{E}^{\diamond -1} = \cos^{\diamond}\gamma$ and $\mathrm{d}r^{\diamond}/\mathrm{d}t^{\diamond} = \sin\gamma$, we have the metric:

$$\frac{1}{t^2}\left(\tau^2 = t^2 - r^2\right) \quad \equiv \quad \left(\frac{mc^2}{\mathbb{E}}\right)^2 = 1 - v^2 = \tag{14i}$$

$$= \frac{1}{\cosh^2\zeta} = 1 - \tanh^2\zeta = \tag{14j}$$

$$= \frac{(\mathbb{E}^{\diamond}/mc^2)^{-2}}{(E/mc^2)^2} = 1 - \frac{1}{(E/mc^2)^2} b_{\Gamma/2}^2 \left(\frac{\mathrm{d}r^{\diamond 2}}{c^2\mathrm{d}t^{\diamond 2}}\right) = \tag{14k}$$

$$= c^2\mathrm{d}t^{\diamond 2} = \frac{E^2}{m^2c^4}\frac{c^2\mathrm{d}t^{\diamond 2}}{(\mathbb{E}^{\diamond}/mc^2)^{-2}} - b_{\Gamma/2}^2 \frac{\mathrm{d}r^{\diamond 2}}{(\mathbb{E}^{\diamond}/mc^2)^{-2}} - \left[b_{\Gamma/2}^2 r^{\diamond 2}\mathrm{d}\Omega^2\right] \tag{14l}$$

It is now easy to recognize, in the (14l), the Schwarzschild metric in free fall, where the only difference is the exchange of $\tau^{\diamond}$ with $t^{\diamond}$ and the presence of the factor $b_{\Gamma/2}$.

2.1.2 Centrally symmetric Force Field ($\mathrm{d}R_m = 0$)

In the instant there is no difference between an inertial system and a system immersed in a force field, since the metric is determined, point by point, solely by the local rotation angle γ and this in turn depends solely on the nature of the Radii of the bodies involved.

In a Force Field, unlike what happens in an inertial system, it is the Radius that is constant and not the γ angle. This, in a static system, in light of the unique interaction scheme (see fig. A5), has two important consequences:

$$\mathrm{d}r_{S\,chwarz.} = \mathrm{d}(b_{\Gamma/2}\, r^{\diamond}) = \mathrm{d}(r^{\diamond} - R_m/2) = \mathrm{d}r^{\diamond} \tag{15}$$

$$\frac{\mathbb{E}^{\diamond}_{force\,field}}{mc^2} = \cos^{\diamond}\gamma = \left(\frac{\mathbb{E}^{\diamond}_{inertial}}{mc^2}\right)^{-1} \tag{16}$$

That is, due to the constancy of the radius R_m, the term $\sin\gamma$, present in the factor $b_{\Gamma/2}$, constant in the inertial system, in the force field is instead inversely proportional to the distance, i.e. equal to $V^{\diamond} = R_m/r^{\diamond}$ whence the (15). This same constancy of the radius acts on the scheme causing the inversion between $t^{\diamond}$ and $\tau^{\diamond}$ whence the (16). Furthermore, as will be demonstrated in the next section 2.1.3, the ratios between proper and frame coordinates are the same for both Schwarzchild and linear coordinate systems, that is:

$$g_{00} = 1/g_{rr} = 1 - 2V = \left(1 - V^{\diamond}\right)^2 = \left(\frac{\mathbb{E}^{\diamond}}{mc^2}\right)^2 \tag{17}$$

Summing up, since $\mathrm{d}R_m = 0$, the differential Schwarzchild coordinates, used by GTR, coincide with the linear ones of the IRPL space and not with the Minkowski ones used by SR:

$$\mathrm{d}\tau_{S\,chwarz.} \equiv \mathrm{d}\tau^{\diamond} \qquad \mathrm{d}\sigma^{\diamond} \equiv \mathrm{d}\sigma_{S\,chwarz.} \qquad \mathrm{d}t^{\diamond} \equiv \mathrm{d}t_{S\,chwarz.} \qquad \mathrm{d}r^{\diamond} \equiv \mathrm{d}r_{S\,chwarz.} \tag{18}$$

and

$$\frac{\mathbb{E}^{\diamond}}{mc^2} = \cos^{\diamond}\gamma \qquad\qquad V^{\diamond} = \frac{R_m}{r^{\diamond}} = \frac{\mathrm{d}r^{\diamond}}{\mathrm{d}\tau^{\diamond}} = p^{\diamond}/mc = \sin^{\diamond}\gamma \tag{19}$$

where $\pi \leq \gamma \geq 0$ for attractive force fields, the complement for the repulsive ones; $|\gamma| \leq \pi/2$ outside the Radius, $|\gamma| \geq \pi/2$ inside.

The energy term E/mc^2, present in the (14l), actually represents a conversion factor. Indeed, its presence is the sign that reveals a forcing, i.e. the constraint of linear coordinates in a quadratic form. Similarly, along the lines of the (14l), we look for the local frame in Minkowski spacetime homomorphic to the linear one, that is with $v = \mathrm{d}r/\mathrm{d}t = v^{\diamond} = \mathrm{d}r^{\diamond}/\mathrm{d}t^{\diamond}$ being $\tau \equiv \tau^{\diamond}$. In other words:

$$\frac{\mathrm{d}r^{\diamond}}{i\,\mathrm{d}r} = \frac{\mathrm{d}t^{\diamond}}{\mathrm{d}t} = \frac{E}{mc^2} \qquad \left(\frac{p^{\diamond}}{i\,p} = \frac{\mathbb{E}^{\diamond}}{\mathbb{E}} = \frac{E}{mc^2}\right) \tag{20}$$

from which it follows:

$$\frac{E}{mc^2} = \pm\sqrt{\left(\frac{\mathbb{E}^\diamond}{mc^2}\right)^2 + \left(\frac{p^\diamond}{mc}\right)^2} \qquad \frac{\mathbb{E}}{mc^2} = \cos\xi = \frac{\mathbb{E}^\diamond}{E} \qquad i\,\frac{p}{mc} = \sin\xi = \frac{cp^\diamond}{E} \tag{21}$$

The (20) allows the translation of the quadratic or Minkowski coordinates (t, r) into the linear or Schwarzchild ones $(t^\diamond, r^\diamond)$ and, consequently, the translation of the metric between one system and another. That is :

$$\mathrm{d}t^2 = \mathrm{d}\tau^2 + \mathrm{d}r^2 \tag{22a}$$

$$\equiv \frac{\mathrm{d}t^{\diamond 2}}{(E/mc^2)^2} = \mathrm{d}\tau^{\diamond 2} - \frac{\mathrm{d}r^{\diamond 2}}{(E/mc^2)^2} \tag{22b}$$

$$\equiv \frac{\mathrm{d}\tau^{\diamond 2}(\mathbb{E}^\diamond/mc^2)^2}{(E/mc^2)^2} = \mathrm{d}\tau^{\diamond 2} - \frac{\mathrm{d}r^{\diamond 2}}{(E/mc^2)^2} \tag{22c}$$

$$\equiv \mathrm{d}\tau^{\diamond 2} = (E/mc^2)^2\frac{\mathrm{d}\tau^{\diamond 2}}{(\mathbb{E}^\diamond/mc^2)^2} - \frac{\mathrm{d}r^{\diamond 2}}{(\mathbb{E}^\diamond/mc^2)^2} - \left[r^{\diamond 2}\mathrm{d}\Omega^2\right] \tag{22d}$$

Note that the (21) implicitly includes the motion constant and unmasks the term $E = \mathbb{E}^\diamond/\mathbb{E}$ present in the free fall Schwarzchild metric (22d), highlighting that it represents a conversion factor and unifying the expression of the true energy, which is always equal to the ratio between frame coordinate time and proper time.

In the circular motion, the time axes of the two involved individuals, in addition to the rotation angle γ in the pseudo-plane of the act, rotate by an angle ϑ in the plane of potency. Since the equivalence of potential and momentum:

$$V^\diamond \equiv \frac{R}{r^\diamond} \equiv \frac{\mathrm{d}r^\diamond}{c\mathrm{d}\tau} \equiv \frac{L/mc}{r^\diamond} \tag{22e}$$

we have at last

$$\frac{1}{2}mc^2\left(1 - \frac{E^2}{m^2c^4}\right) = mc^2\left(V^\diamond - \frac{1}{2}V^{\diamond 2} - \frac{1}{2}\frac{\mathrm{d}r^{\diamond 2}}{c^2\mathrm{d}\tau^2} - \frac{1}{2}\frac{L^2}{m^2c^2r^{\diamond 2}}\left(1 - V^\diamond\right)^2\right) \tag{22f}$$

formulas (14l) and (22d) turn into each other with the exchange of $t^\diamond$ with $\tau^\diamond$.

2.1.3 Derivation of the Schwarzschild metric

In the previous sections, to equal the Schwarzschild metric to the linear one, it was necessary to hire:

$$g_{00} = 1/g_{rr} = 1 - 2V = \left(1 - V^\diamond\right)^2 = \left(\frac{\mathbb{E}^\diamond}{mc^2}\right)^2 \tag{23}$$

which implies the following relation between the Schwarzschild potential V and the linear potential $V^{\diamond}$:

$$V = V^{\diamond}\left(1 - \frac{V^{\diamond}}{2}\right) \tag{24}$$

This difference is due to the fact that, unlike the linear potential $V^{\diamond}$, the Schwarzschild potential arises not from the intrinsic mass (proper mass) of the two individuals involved, but from the masses immersed in their resulting field $\mathbb{E}^{\diamond} = \cos^{\diamond}\gamma$ as seen by a far away observer. That is, the global Radius R_2 that creates the field, seen by a far away observer and employed by the Schwarzschild potential, is given by half of the sum of the Radius of A in the field of B, i.e. $R_{2_{Ba}} = 2\left(R_b + R_a\cos^{\diamond}\gamma\right)$, and of the Radius of B in the field of A, i.e. $R_{2_{Ab}} = 2\left(R_a + R_b\cos^{\diamond}\gamma\right)$. Therefore, denoting with $R = G/c^2(m_a + m_b)$, we have :

$$R_2 = 2R\frac{1+\cos^{\diamond}\gamma}{2} = 2R\,b_{\Gamma/2} = 2R\left(1 - \frac{V^{\diamond}}{2}\right) \qquad V = \frac{\frac{1}{2}R_2}{r^{\diamond}} = V^{\diamond}\left(1 - \frac{V^{\diamond}}{2}\right) \tag{25}$$

Indeed, the expression for the energy-momentum tensor in an arbitrary reference system, where u^i is the four-velocity for the macroscopic motion of an element of volume of the body is:

$$T_k^i = (\rho + p)u_i u^k - p\delta_i^k \tag{26}$$

where

$$u_0 u^0 = -u_1 u^1 = \frac{1}{1 - v^2/c^2} \qquad\qquad \delta_0^0 = -\delta_1^1 = 1$$

Since $v = 0$, and, from the (8) , $R = r^{\diamond 2}/\tau^{\diamond}$

$$\mathbb{E} = \frac{c^2}{G}\frac{r_s}{2} = \frac{c^2}{G}\frac{r^{\diamond 2}}{\tau^{\diamond}}\left(1 - \frac{\sin\gamma}{2}\right) = \frac{c^2}{G}\frac{r^{\diamond 2}}{\tau^{\diamond}} - \frac{1}{2}\frac{c^2}{G}\frac{r^{\diamond 3}}{\tau^{\diamond 2}} \tag{27}$$

and since

$$\int 4\pi r^{\diamond 2}\rho\left(r^{\diamond}\right)dr^{\diamond} = \mathbb{E} \tag{28}$$

we arrive at the energy density W as

$$W = T_0^0 = \rho\left(r^{\diamond}\right) = \frac{c^2}{8\pi G}\frac{4}{r^{\diamond}\tau^{\diamond}} - \frac{c^2}{8\pi G}\frac{3}{\tau^{\diamond 2}} \tag{29}$$

As usual, to find the universe metric, we start from [see 21, pag 283] :

$$ds^2 = e^{\nu}c^2 dt^{\diamond 2} - r^{\diamond 2}\left(d\theta^2 + \sin^2\theta d\phi^2\right) - e^{-\lambda}dr^{\diamond 2}$$

which gives:

$$\begin{cases} e^{-\lambda}\left(\frac{\nu'}{r^{\diamond}} + \frac{1}{r^{\diamond 2}}\right) - \frac{1}{r^{\diamond 2}} = \frac{8\pi G}{c^4}T_1^1 \\ e^{-\lambda}\left(\frac{\lambda'}{r^{\diamond}} - \frac{1}{r^{\diamond 2}}\right) + \frac{1}{r^{\diamond 2}} = \frac{8\pi G}{c^4}T_0^0 \\ \dot{\lambda} = 0 \end{cases}$$

Since $\lambda = -\nu$ and $T_0^0 = -T_1^1$ we reduce to the only equation:

$$e^{-\lambda}\left(\frac{\lambda'}{r^\diamond} - \frac{1}{r^{\diamond 2}}\right) + \frac{1}{r^{\diamond 2}} = \frac{4}{r^\diamond \tau^\diamond} - \frac{3}{\tau^{\diamond 2}} \tag{30}$$

which admits one solution

$$e^{-\lambda} = \left(1 - \frac{r^\diamond}{\tau^\diamond}\right)^2 \tag{31}$$

Therefore, the metric of universe in the usual general relativity coordinate system (τ, σ, t, r), observer dependent, which correspond to an "accelerated" frame, like that of an observer held at a fixed spatial point in the surrounding spacetime, is:

$$dl^2 = \left(1 - \frac{r^\diamond}{\tau^\diamond}\right)^2 c^2 dt^{\diamond 2} - \frac{dr^{\diamond 2}}{\left(1 - \frac{r^\diamond}{\tau^\diamond}\right)^2} - r^{\diamond 2} d\theta^2 - r^{\diamond 2} \sin^2\theta \, d\phi^2 \tag{32}$$

Or, since $R/r^\diamond = r^\diamond/\tau^\diamond$, that is $V^\diamond = p^\diamond/mc$

$$dl^2 = \left(1 - \frac{R}{r^\diamond}\right)^2 c^2 dt^{\diamond 2} - \frac{dr^{\diamond 2}}{\left(1 - \frac{R}{r^\diamond}\right)^2} - r^{\diamond 2} d\theta^2 - r^{\diamond 2} \sin^2\theta \, d\phi^2 \tag{33}$$

Denoted by R_{ind} the Radius of an individual, we will use the eq. (32) inside R_{ind}, where $\tau^\diamond = R_{ind}$ is constant and the cold dark matter gives place to $R = r^{\diamond 2}/\tau^\diamond \leq R_{ind}$, the eq. (33) outside R_{ind}, where $R = R_{ind}$ is constant (as long as the cdm of the universe is still negligible) and $\tau^\diamond = r^{\diamond 2}/R_{ind} \leq c/H_0$.

3 Cosmology on the path of light

About the fig. (1)

- the vector $r^\diamond$ is the radial distance in the linear coordinates system $r^\diamond = c\left(\tau^\diamond_{receiving} - t^\diamond_{sending}\right)$, where $\tau^\diamond$ and $t^\diamond$ are the proper time starting (with zero) from the point of minimum distance;
- the vectors R_0 represents the Hubble time $R_0 = c/H_0$ now, at the instant of reception. The vector $h^\diamond$ represents the Hubble time at the instant of emitting.

Therefore:

$$\vec{r}^\diamond + \vec{h}^\diamond = \vec{R}_0 \qquad \sin\gamma + \cos^\diamond\gamma = 1 \tag{34a}$$

$$r^\diamond = \sin\gamma R_0 \qquad h^\diamond = \cos^\diamond\gamma R_0 = (1 - \sin\gamma) R_0 \tag{34b}$$

and

$$\mathrm{d}h^\diamond = R_0(1 - \sin\gamma)\mathrm{d}\gamma \qquad \mathrm{d}r^\diamond = -R_0(1 - \sin\gamma)\mathrm{d}\gamma \qquad \mathrm{d}h^\diamond = -\mathrm{d}r^\diamond \tag{34c}$$

and

$$a^{\diamond}(\gamma) = \frac{\lambda_{emitted}}{\lambda_{received}} = \frac{h^{\diamond}}{R_0} = (1 - \sin\gamma) \quad \equiv \quad a(t) = \frac{1}{1+z} \quad \textit{the scale factor} \tag{34d}$$

and, from the eq (34d)

$$\gamma = \arcsin\frac{z}{z+1} \qquad\qquad z = \frac{1}{1-\sin\gamma} - 1 \tag{34e}$$

and from the (14c) and the equivalence between inertial and force fields, the equivalence of the three redshifts:

$$\text{Gravitational redshift} \quad \frac{\mathbb{E}^{\diamond}_{inertial}}{mc^2} = \left(\frac{\mathbb{E}^{\diamond}_{forcefield}}{mc^2}\right)^{-1} = \frac{1}{1-\sin\gamma} = 1+z \tag{35}$$

$$\text{Doppler redshift} \quad \sqrt{\frac{1+v}{1-v}} = \frac{1}{1-\sin\gamma} = 1+z \tag{36}$$

$$\text{FLRW redshift} \quad \frac{R_0}{h^{\diamond}} = \frac{1}{a} = \frac{1}{1-\sin\gamma} = 1+z \tag{37}$$

Before addressing the universe metric it is necessary to make a hypothesis.

3.1 The cosmological hypothesis

Cosmology is based on Einstein's field equations, Friedmann equations and FLRW metric. These in turn derive from the IRPL space which, since cosmology begins when $\tau^{\diamond} = \tau^{\diamond}_{max} = R_0 = R_{\Omega}$, on the basis of the hypothesis (1) asserts the fundamental cosmological relation (8)

$$V^{\diamond} = \frac{R_m}{r^{\diamond}} = \sin\gamma = \frac{r^{\diamond}}{R_0} = p^{\diamond}/mc \tag{38}$$

From the (38) it directly follows the thesis:

Thesis 2 *In the relationship between an observer-observed pair in the Universe, the total gravitational radius* $R_m = R_{observer} + R_{observed}$ *grows proportionally to the radial distance. More precisely:*

$$R_m = \sin^2\gamma R_{\Omega} = \sin\gamma \cdot r^{\diamond} \tag{39}$$

The (39) conforms to, and support, the holographic principle and the first law of black hole mechanics [34–36].

At last, to match the results of the observations, it is necessary to introduce the further hypothesis:

Hypothesis 2 *the light path between an emitter and a receiver has an extra path in the total Radius of the observer and observed, so that, in a free falling frame, we have:*

$$r^{\diamond}_{observed} = \int \mathrm{d}r^{\diamond} + R_m = r^{\diamond} + V^{\diamond}\, r^{\diamond} = b_{\Gamma} \int \mathrm{d}r^{\diamond} \tag{40}$$

where $V^{\diamond}(\gamma)$ is the potential between the sender and the receiver and $b_{\Gamma} = \left(1 + V^{\diamond}\right)$ the Rpath factor.

Note that the Rpath factor b_{Γ} is constant along the path of integration. The cosmological hypothesis (2), nevertheless, is based on considerations of a geometric nature on the scheme of the universal relationship (see appendix A).

3.2 The metric of the universe for itself (neglecting the extra path in the Radius)

The FLRW metric was derived by neglecting the extra path due to the radius of observer and observed inside the universe. Consequently, on the basis of hypothesis (2), it represents the universe for itself, not the one observed from an internal point. An internal observer, in fact, would inexorably have a mass depending on the observed distance which would add to the distance to be measured.

The equations that describe the time evolution of an expanding universe which is homogeneous and isotropic can be deduced stating from the (32)

$$c^2\mathrm{d}\tau^2 = c^2\mathrm{d}t^{\diamond 2}\left(1 - V^{\diamond}\right)^2 - \frac{\mathrm{d}r^{\diamond 2}}{(1 - V^{\diamond})^2} - r^{\diamond 2}\mathrm{d}\boldsymbol{\Omega}^2 \tag{41}$$

and, since for matter in free fall the constant of motion $\mathrm{d}t^{\diamond} = E/mc^2 \frac{\mathrm{d}\tau}{(1-V^{\diamond})^2}$ holds, we have:

$$c^2\mathrm{d}\tau^2 = E^2/m^2c^4 \frac{c^2\mathrm{d}\tau^2}{(1 - V^{\diamond})^2} - \frac{\mathrm{d}r^{\diamond 2}}{(1 - V^{\diamond})^2} - r^{\diamond 2}\mathrm{d}\boldsymbol{\Omega}^2 \tag{42}$$

Although both may be derived from the same Schwarzschild metric, the FLRW metric follows the path of light between a sending-receiving pair and shows how does the distance vary as γ varies for a given time. Friedmann's equations, contrariwise, follow the time evolution of universe in free fall in its own force field and shows how does the expansion vary as τ varies for a given γ.

In a homogeneous universe every particle moving with the substratum has a purely radial velocity proportional to its distance from the observer. We can therefore change to a more convenient coordinate system, known as comoving coordinates. These are coordinates that are carried along with the expansion $a(t)$,

$$x = a_{(t)}\, r^{\diamond} \qquad y = a_{(t)} t^{\diamond} \qquad \dagger = a_{(t)}\tau \tag{43a}$$

therefore we can then change to comoving coordinates by multiplying each member of the (42) by $a_{(t)}$

$$\mathrm{d}\dagger^2 = E^2/m^2c^4 \frac{\mathrm{d}\dagger^2}{(1 - V^{\diamond})^2} - \frac{\mathrm{d}x^2}{(1 - V^{\diamond})^2} - x^2\mathrm{d}\boldsymbol{\Omega}^2 \tag{43b}$$

Birkhoff's theorem states that the net gravitational effect of a uniform external medium on a spherical cavity is zero - in other words, the force acting on the edge of a sphere of radius x is the gravitational attraction from the matter M internal to x only, which acts as a point mass at center O.

Dividing each member of (43b) by $\mathrm{d}\dagger^2$

$$1 = \frac{E^2/m^2c^4}{(1 - V^{\diamond})^2} - \frac{\dot{x}^2}{(1 - V^{\diamond})^2} \tag{43c}$$

and then multiplying each member by $(1 - V^{\diamond})^2$, we get the total energy of a particle of mass m at the edge of a sphere as the usual sum of kinetic and gravitational potential energy

$$U = T + V = \frac{1}{2}m\dot{x}^2 - \frac{GMm}{x} = \frac{1}{2}m\dot{x}^2 - \frac{4\pi}{3}G\rho x^2 m \tag{43d}$$

where the dot denotes differentiation with respect to $\dagger$, ρ is the density of matter within the sphere of radius x, and G is Newton's gravitational constant. Substituting (43a) into (43d) we have:

$$U = \frac{1}{2}m\dot{a}^2 r^{\diamond 2} - \frac{4\pi}{3}G\rho a^2 r^{\diamond 2} m \tag{43e}$$

which can be re-arranged into the familiar form of the Friedmann equation

$$H^2 = \left(\frac{\dot{a}}{a}\right)^2 = \frac{8\pi}{3}G\rho - \frac{kc^2}{a^2} \tag{43f}$$

where

$$kc^2 = -\frac{2U}{mr^{\diamond 2}} \tag{43g}$$

and

$$\frac{U}{mc^2} = \frac{1}{2}\left(\left(\frac{E}{mc^2}\right)^2 - 1 - V^{\diamond 2}\right) \tag{43h}$$

Note that k must be independent of $r^{\diamond}$, since the other terms in the equation are. Thus $U \propto r^{\diamond 2}$; homogeneity requires that U, while constant for a given particle, does change if we look at different comoving separations $r^{\diamond}$. From eq. (43g) we can also see that $k \neq f(\dagger)$, since for a given particle the total energy U is conserved and $\dot{r}^{\diamond} = 0$ by definition. Thus k is just a constant, unchanging with either space or time. Therefore, for the universe it must hold:

$$\frac{E}{mc^2} = 1 \tag{43i}$$

and [1]

$$\frac{U}{mc^2} = -\frac{1}{2}V^{\diamond 2} = -\frac{1}{2}\frac{r^{\diamond 2}}{R_0^2} \tag{43j}$$

and at last

$$k = \frac{1}{R_0^2} = \left(\frac{H_0}{c}\right)^2 \tag{43k}$$

An expanding universe has a unique value of k which it maintains throughout its evolution. The value of k determines the form of this evolution. A positive k implies negative U, so that $V > T$ in eq. (43d) - the expansion will at some time t_{halt} halt and reverse itself. Since in the IRPL model there is not dark energy and, thanks to CDM, $R_\Omega = R_0$ or equivalently $\rho_0 = \rho_{critic}$, then the universe, for itself, is closed with positive curvature radius and negative surface gravity equal to H_0/c, and is now stopping and reversing itself $t_0 = t_{halt}$.

Since the (43i), the (42) become:

$$\mathrm{d}s^2 = \frac{c^2\mathrm{d}\tau^2}{(1-V^\diamond)^2} - \frac{\mathrm{d}r^{\diamond 2}}{(1-V^\diamond)^2} - r^{\diamond 2}\mathrm{d}\boldsymbol{\Omega}^2 \tag{44a}$$

About the mapping between Schwarzschild and FLRW coordinates, from the homomorphic relations (20), which require $\mathrm{d}r/\mathrm{d}\mathbb{E} = \mathrm{d}r^\diamond/\mathrm{d}\mathbb{E}^\diamond$, we have:

$$\mathrm{d}\sigma_{FLRW} = \frac{\mathrm{d}r_{FLRW}}{\sqrt{1-\frac{r_{FLRW}^2}{R_0^2}}} = \mathrm{d}\sigma^\diamond = \frac{\mathrm{d}r^\diamond}{1-V^\diamond} \qquad \mathrm{d}\tau_{FLRW} = \mathrm{d}\tau^\diamond \tag{44b}$$

At last, since $\mathrm{d}r^\diamond = R_0\mathrm{d}V^\diamond = R_0(1-V^\diamond)\mathrm{d}\gamma$ and $a_{(\tau)} = (1-V^\diamond)$, both the (42) and the FLRW metric converge at:

$$\mathrm{d}s^2 = \frac{c^2\mathrm{d}\tau^2}{a_{(\tau)}^2} - R_0\mathrm{d}\gamma^2 - r^{\diamond 2}\mathrm{d}\boldsymbol{\Omega}^2 \tag{44c}$$

where $r^\diamond$ is the Schwarzschild radial coordinate. Usually t is used for the cosmic time variable instead of τ.

3.3 The metric of the universe actually seen by the observer

To get the metric of the universe actually seen by an observer inside the universe, it is necessary to take into account the extra path in the Radius of the observer-observed matter by multiplying each member of (44c) by b_Γ. The $\mathcal{M}$etric of universe at last

[1] $E/mc^2 = 1$ when $\mathbb{E}^\diamond = 1$, $p^\diamond/mc = 0$ ($\gamma = 0$) or when $\mathbb{E}^\diamond = 0$, $p^\diamond/mc = 1$ ($\gamma = \pi/2$).

becomes:

$$ds^2 = \frac{c^2 dt^2}{a\,(t)^2} - b^2\,(\gamma)\left(R_0^2 d\chi^2 + r^{\diamond 2} d\theta^2 + r^{\diamond 2}\sin^2\theta d\phi^2\right) \tag{45}$$

where

$$\mathrm{d}d_M = b(\gamma)\frac{\mathrm{d}r^{\diamond}}{A^{\diamond}(r^{\diamond})} = -b(\gamma)\,R_0\mathrm{d}\chi \qquad\qquad c\frac{\mathrm{d}t}{a(t)} = b(\gamma)\,R_0\mathrm{d}\chi \tag{46}$$

Since $\Omega_0 \approx 1$ from observations and the IRPL model does not contemplate the cosmological constant, we have $\Omega_{0_m} = \Omega_{0_b} + \Omega_{0_c} \approx 1$. Therefore, provisionally neglecting the radiation

$$d_M = b(\gamma)\int_0^{\gamma} R_\omega d\chi = b(\gamma)\cdot\frac{c}{H_0}\gamma = \frac{c}{H_0}\gamma + R_m(\gamma) \tag{47}$$

That is:

$$d_M = b(\gamma)\int_0^{\gamma} R_\omega d\chi = \frac{c}{H_0}\,(1+\sin\gamma)\,\gamma \quad = \frac{c}{H_0}\left(1+\frac{z}{z+1}\right)\arcsin\left(\frac{z}{z+1}\right) \tag{48a}$$

$$d_A = a d_M = \frac{c}{H_0}\left(1-\sin^2\gamma\right)\gamma \quad = \frac{c}{H_0}\frac{(2z+1)}{(z+1)^2}\arcsin\left(\frac{z}{z+1}\right) \tag{48b}$$

$$d_L = \frac{d_A}{a^2} = \frac{c}{H_0}\frac{1+\sin\gamma}{1-\sin\gamma}\gamma \quad = \frac{c}{H_0}\,(2z+1)\arcsin\left(\frac{z}{z+1}\right) \tag{48c}$$

At this point it should be pointed out that the increase $\mathrm{d}d_M$ (see eq. 46) represents the progressive advancement in the path $\mathrm{d}\chi$ between a predetermined sender-receiver pair whose distance Γ remains fixed. In other words, the extra path $\mathrm{d}R_m \propto \mathrm{d}r^{\diamond}$, where the multiplicative coefficient $V^{\diamond} = \sin\gamma$ is constant and depends on the angle γ of the path between the sender-receiver pair. In the FLRW metric, on the contrary, the increment of the path coincides with the increment of the distance $\mathrm{d}\chi \equiv \mathrm{d}\gamma$.

Therefore, when $\mathrm{d}\chi \equiv \mathrm{d}\gamma$, the increase $\mathrm{d}d_M$ and $\mathrm{d}z$ along the Line Of Sight become:

$$\mathrm{d}d_M = \frac{c}{H_0}(1+\sin\gamma+\gamma\cos\gamma)\mathrm{d}\gamma \tag{48d}$$

$$dz = \frac{\cos\gamma}{(1-\sin\gamma)^2}d\gamma = \sqrt{(1+\sin\gamma)\,a^{-3}}\,d\gamma = \sqrt{2a^{-3}-a^{-2}}\,d\gamma \tag{48e}$$

Now, it is critical to point out that the (43f) is expressed as a function of $\dagger^{\diamond}$. In other words, $\dot{a}$ stands for $\mathrm{d}a/\mathrm{d}\dagger^{\diamond} = \mathrm{d}a/\mathrm{d}t\cdot\mathrm{d}t/\mathrm{d}\dagger^{\diamond}$. Now, since $\mathrm{d}t = a\,\mathrm{d}d_M/\mathrm{d}\gamma\cdot\mathrm{d}\gamma$ and $\mathrm{d}\dagger^{\diamond} = R_0\,a\,\mathrm{d}\gamma$, we have that

$$H_{(t)} = \frac{\mathrm{d}\dagger^{\diamond}}{\mathrm{d}t}\cdot H_{(\dagger^{\diamond})} = \frac{R_0}{d'_{M(\gamma)}}\cdot H_{(\dagger^{\diamond})} \tag{48f}$$

and therefore the (43f) becomes:

$$H^2 = \left(\frac{\dot{a}_{(t)}}{a_{(t)}}\right)^2 = R_0^2 \frac{8\pi/3\, G\rho - kc^2 a_{(t)}^{-2}}{(\mathrm{d}d_M/\mathrm{d}\gamma)^2} = \frac{8\pi/3\, G\rho - kc^2 a_{(t)}^{-2}}{(1+\sin\gamma+\gamma\cos\gamma)^2} \tag{48g}$$

and

$$H = \frac{\mathrm{d}z}{\mathrm{d}d_M} = \frac{\mathrm{d}\gamma}{\mathrm{d}d_M}\frac{\mathrm{d}z}{\mathrm{d}\gamma} = H_0 \sqrt{\Omega_{0_m} \frac{(1+\sin\gamma)}{(1+\sin\gamma+\gamma\cos\gamma)^2}\, a^{-3}} = H_0 \sqrt{\frac{\Omega_{ms}(\gamma)}{a^{-3}}} \tag{48h}$$

$$t = \int_0^{\gamma} \frac{a}{H(z)} \mathrm{d}z \tag{48i}$$

where $\Omega_{ms}(\gamma)$ is the sum of the two components:

$$\Omega_m(\gamma) = \frac{\Omega_{0_m}}{(1+\sin\gamma+\gamma\cos\gamma)^2} \qquad \Omega_s(\gamma) = \frac{\Omega_{0_m}\,\sin\gamma}{(1+\sin\gamma+\gamma\cos\gamma)^2} \tag{48j}$$

We will indicate this second term, i.e. Ω_s, with the name of "shadow matter". It is assumed to be a fictitious mass of a different nature from proper mass. The "shadow matter", in turn, breaks down into two components:

$$\Omega_s(\gamma) = \Omega_{0_m} \frac{\mathbf{1} - (1-\sin\gamma)}{(1+\sin\gamma+\gamma\cos\gamma)^2} = \Omega_h(\gamma) + \Omega_k(\gamma)\, a(\gamma) \tag{48k}$$

$$\Omega_m = \Omega_h = -\Omega_k \tag{48l}$$

Indeed the universe is finite and has a positive spatial curvature $R_0 = \frac{c/H_0}{\sqrt{2-\Omega_0}}$.

Already with this first approximation, we obtain results almost identical to those of the ΛCDM model but not in the radiation dominated era.

This divergence is closed when the last ingredient of the Universe, i.e. radiation, is also taken into account so that $\Omega_0 = \Omega_{0_m} + \Omega_{0_r} = 1$

$$H(\gamma) = H_0 \sqrt{\frac{\Omega_{0_r}}{a^4(\gamma)} + \frac{\Omega_{ms}(\gamma)}{a^3(\gamma)}} = H_0 \sqrt{\rho_r + \rho_m + \rho_s} \tag{49a}$$

$$d_M = \int_0^z \frac{c\, dz}{H_0 \sqrt{\frac{\Omega_{0_r}}{a^4(t)} + \frac{1+\sin\gamma}{(1+\sin\gamma+\gamma\cos\gamma)^2}\frac{\Omega_{0_m}}{a^3(t)}}} \tag{49b}$$

Furthermore, the present model does not need end therefore does not contemplate dark energy. Indeed the cosmological factor b_Γ gives rise to a fictitious matter pressure which, alone, gives reason for all the acceleration in the expansion of the universe.

Indeed, starting from the above density formulas, since, using the first equation of Friedmann equations (4), the second equation (5) can be re-expressed as:

$$\dot{\rho} = -3\frac{\dot{a}}{a}\left(\rho + \frac{p}{c^2}\right) \qquad \text{or} \qquad \frac{p}{c^2} = -\left(\frac{1}{3}\frac{a}{\dot{a}}\dot{\rho} + \rho\right) \tag{50}$$

where the ρ includes the shadow matter, i.e. $\rho = \rho_r + \rho_m + \rho_s$, and the pressure, consequently, the shadow pressure. Since, from the (1), $dt = ad'_M(\gamma)d\gamma$ and $da = -\cos\gamma d\gamma$, we find the three components of pressure $p(t) = p_r(t) + p_m(t) + p_s(t)$:

$$\frac{p_r(t)}{c^2} = \rho_{crit}\frac{1}{3}\Omega_r a_{(t)}^{-4} = \frac{\rho_r(t)}{3} \tag{51a}$$

$$\frac{p_m(t)}{c^2} = -\frac{2}{3}\frac{2\cos\gamma - \gamma\sin\gamma}{1 + \sin\gamma + \gamma\cos\gamma}\frac{1}{\cos\gamma}\cdot a_{(t)}\rho_m(t) \tag{51b}$$

$$\frac{p_s(t)}{c^2} = \sin\gamma\cdot\frac{p_m(t)}{c^2} + \frac{1}{3}\cdot a_{(t)}\rho_m(t) \tag{51c}$$

When $t \to t_0$, that is $\gamma \to 0$ or $a(t) = a(\gamma) \to 1$, we have that the proper matter pressure becomes negative and equal in magnitude to its positive energy density:

$$\lim_{t\to t_0}\frac{p_{ms}(t)}{c^2} = -\rho_m(t_0) \tag{52a}$$

and, from the (5), the acceleration in the expansion of the universe becomes positive (see fig. 2):

$$\lim_{t\to t_0}\frac{\ddot{a}_{(t)}}{a_{(t)}} = -\frac{4\pi G}{3}\left(\rho_r(t_0) + \rho_m(t_0) + 3\left(\frac{\rho_r(t_0)}{3} - \rho_m(t_0)\right)\right) \simeq \frac{R_\Omega}{R_0^3} = (cH_0)^2 \tag{52b}$$

In summary, the fundamental difference with respect to the standard model is given by the factor b_Γ. The cosmological factor b_Γ has dramatic impact on the metric. In fact, it implies that, even if the total amount of energy and matter in the Universe remains constant and equal to R_ω, space varies instead with a law different from the simple cube of distance. As well as in the ΛCDM model, also in the present model $\Omega_{0_m} = \Omega_{0_b} + \Omega_{0_c}$ where Ω_{0_b} represents the baryonic density now and Ω_{0_c} the Cold Dark Matter (CDM) density now. However, they are not constant but vary with redshift z.

The purpose of this article is to demonstrate that the IRPL cosmology finally satisfies all constraints deriving from cosmological observations.

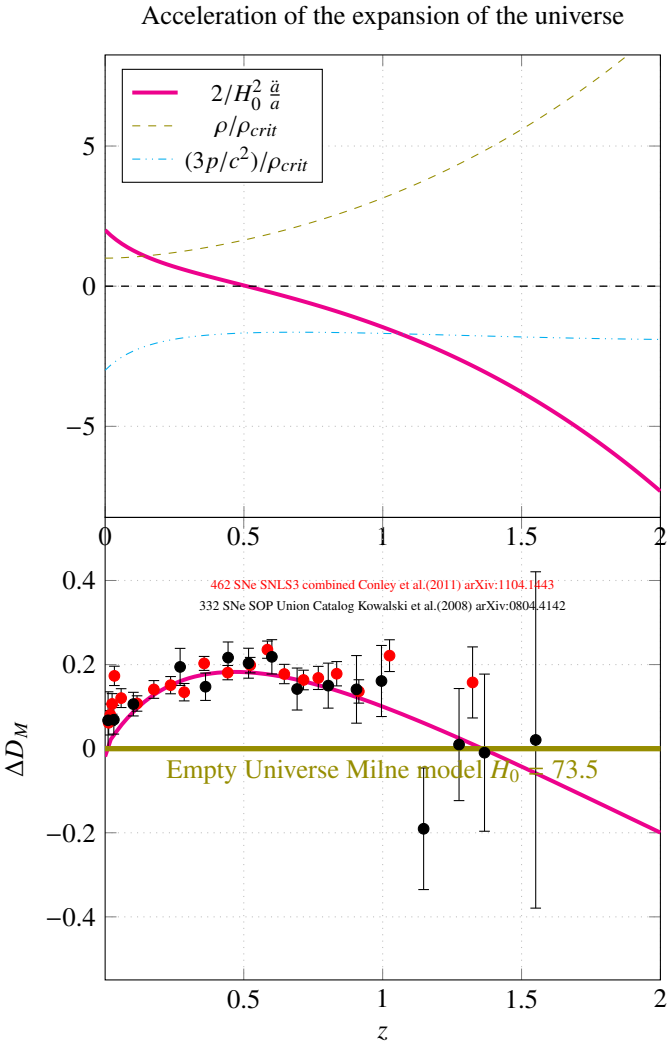

Fig. 2 The top panel shows the pressure $3p/c^2 = \rho_r + \rho_m - \rho_s - 2\cos\gamma\dfrac{d''_M(\gamma)}{d'_M(\gamma)}\rho_m$, the density $\rho = \rho_r + \rho_m + \rho_s$ and the acceleration $\dfrac{2}{H_0^2}\dfrac{\ddot{a}}{a} = \dfrac{-1}{\rho_{crit}}\left(\rho + 3p/c^2\right)$ in the expansion of the universe.
On the bottom panel, the brightness or faintness of distant supernovae relative to the empty Universe model $\Omega = 0$ (the green curve) is plotted vs redshift. The blue-red curve, $\Delta(d_M) = 5\log_{10}\left(\dfrac{d_L}{R_\omega z\left(1+\frac{z}{2}\right)}\right)$ is the difference between the distance modulus determined from the computed flux $d_L = d_M(1+z)$ and the distance modulus computed from the redshift in the empty Universe model. The Hubble constant used in computing the empty Universe Milne model which is subtracted off is 73.5 km/sec/Mpc, and not 63.8 as in Riess et al. (2007).

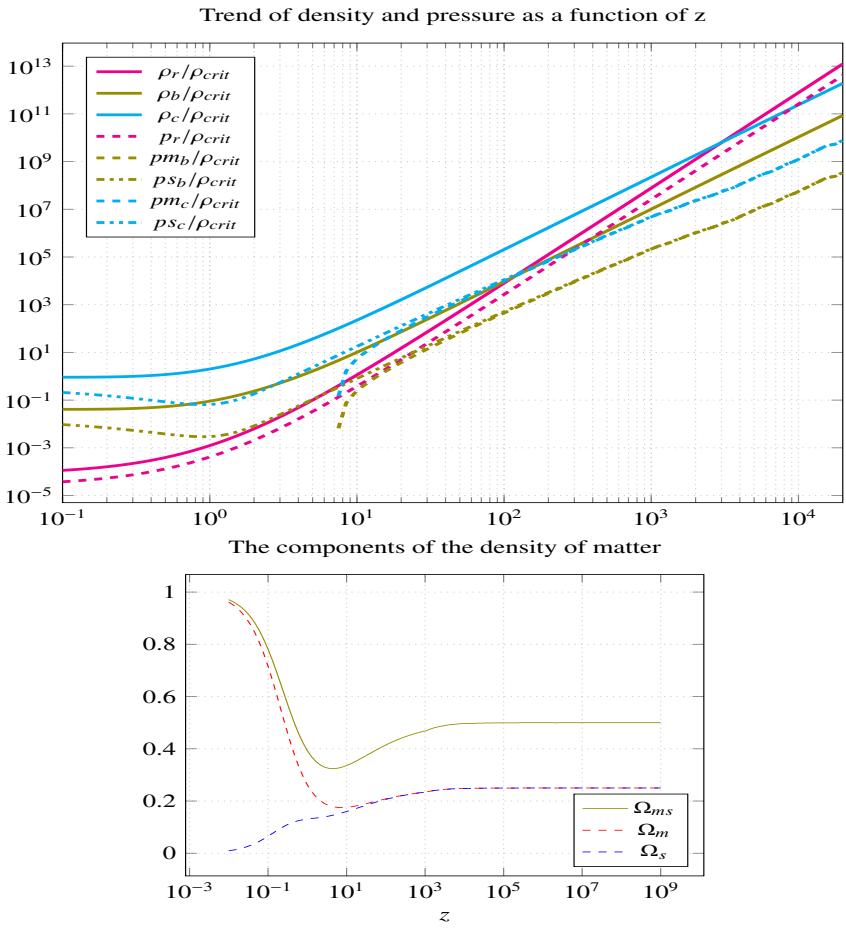

Fig. 3 On the top panel, the trend of density and pressure. On the bottom panel, the density of matter and its two components.

4 Impacts of the IRPL hypothesis on standard cosmology

Since $\Omega_c = 1 - \Omega_r - \Omega_b$, the IRPL Model is determined by only five of the six parameters of the ΛCDM model:

$$\omega_{b_0}, h, n_s, \tau, N_{eff} \tag{53}$$

At last, since the radiation density is precisely determined by the CMB temperature and by the physics of the standard model, the metric of the IRPL Model (eq. (49) is determined by a single parameter:

$$\mathcal{M}(H_0)$$

As densities vary with redshift, it is important to bear in mind that, unlike the ΛCDM model, in the IRPL model we must use the appropriate value of the density of matter according to the cosmological context.
In order to highlight the actual causal region on a case-by-case basis, we have:

- acoustic waves dynamic: CMB temperature and polarization anisotropies are determined not only by the metric but also by the speed of acoustic wave and by the Baryon drag which depend only on the matter component.
  The causal region, however, differs between the following two cases:
  - speed of acoustic wave c_s : the causal region is given by the cosmological redshift

$$c_s(z) \equiv c\sqrt{\frac{\dot{P}_\gamma + \dot{P}_{m_b}}{\dot{\rho}_\gamma + \dot{\rho}_{m_b}}} \simeq \frac{c}{\sqrt{3}} \frac{1}{\sqrt{1 + \frac{3\Omega_{b(z)}}{4\Omega_\gamma(1+z)}}} \qquad r_{s_{(z)}} = \int_z^\infty \frac{c_s(z)}{H(z)} dz \tag{54}$$

  - Baryon Loading: momentum density provides extra inertia in the joint Euler equation for the evolution of acoustic wave oscillation. In this case, the causal region is restricted to the distance between baryons with respect to their barycentre given by the angle $\theta_z = \arcsin\left(r_s(z)/D_M(z)\right)$

$$m_{eff} = 1 + R(\theta_z) = 1 + \frac{3\,\Omega_b(\theta_z)}{4\,\Omega_\gamma(1+z)} \tag{55}$$

- BBN: while both the expansion rate of the universe during the BBN and the baryon-to-photon ratio $\eta = 2.7377 \times 10^{-8}\,\omega_{b_0}$ are almost the same for ΛCDM and IRPL model, the baryon density of IRPL is almost one half with respect to ΛCDM. Indeed from the (48j)

$$\Omega_b(BBN) = \Omega_{b_0} \frac{1 + \sin\gamma}{(1 + \sin\gamma + \gamma\cos\gamma)^2} \approx \frac{1}{2}\Omega_{b_0} \tag{56}$$

  consequently, the nuclear reaction rate of the IRPL model is half that of the ΛCDM model.

About the history of the universe, both models basically share the same phases.
In the Radiation-dominated age, although the nucleosynthesis and the dynamics of the acoustic oscillation are different, the expansion rate: $H(a) \simeq H_0\sqrt{\frac{\Omega_r}{a^4}}$ is identical for both models.
The Radiation-Matter transition happened when $H_r = H_m$, or $d'_{M_m} = d'_{M_r}$, that is $\Omega_m(z) = \Omega_r(1+z)$ or:

$$\frac{1 - \sin\gamma\left(z_{eq_m}\right)}{\left(1 + \sin\gamma(z_{eq_m}) + \gamma(z_{eq_m})\cos\gamma(z_{eq_m})\right)^2} = \frac{\Omega_r}{1 - \Omega_r} \tag{57}$$

Contrary to what happens in the radiation dominate era, in the matter dominated era the expansion rate of the universe is quite different (fig. 4).

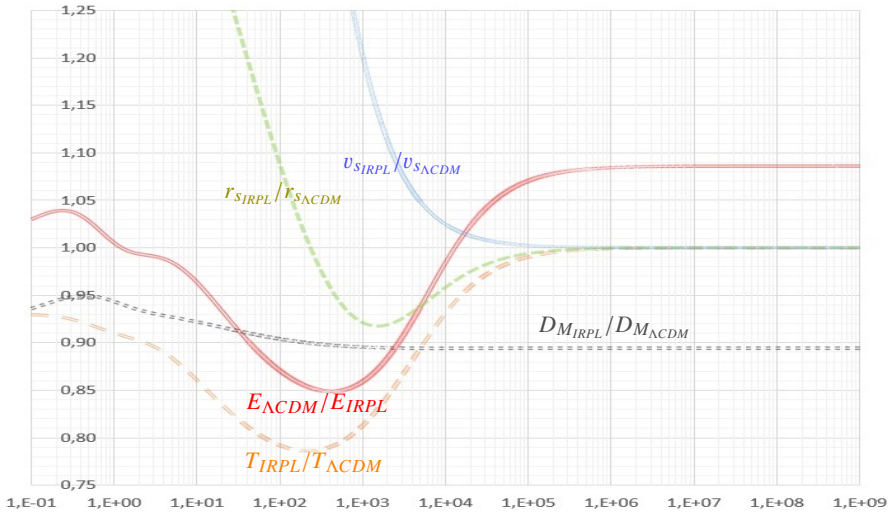

Fig. 4 The scale ratio between the fiducial ΛCDM model ($\omega_b = 0.02242$, $\omega_m = 0.3111$, $H_0 = 67.66$) and the IRPL Model ($\omega_b = 0.02325$, $H_0 = 73.48$). The two models thus configured give rise to an almost identical BAO "Hubble diagram"' (fig. 9)

Furthermore, since there is no Dark Energy in the IRPL model, the matter-dominated era extends to the present and thus encompasses the final era of accelerated expansion of the universe.

5 Constraints on IRPL Cosmological parameters

We determine the last three parameters of the IRPL model and the radiation density as follows:

- The value of the number of effective relativistic degrees of freedom is [2, 6, 13, 16, 17, 22, 39]
$$N_{eff} = 3.044 \tag{58}$$
for 3 neutrino families, taking into account the neutrino decoupling physics. This value is very robust and can be understood fully from the adiabatic transfer of averaged oscillations (ATAO) approximation [16]. This allows one to show that this prediction is insensitive to the type of neutrino mass hierarchy (normal or inverted) as it depends nearly exclusively on mixing angles. Also, since mixing angles are currently known with rather good precision, the propagation of uncertainty affects N_{eff} with $\pm 2 \times 10^{-5}$ only.
- CMB constraints on the scalar spectral index n_s, which describes how the density fluctuations from inflation vary with scale ($n_s = 1$ corresponding to scale invariant fluctuations) [25]
$$n_s = 0.9649 \pm 0.0042 \tag{59}$$
- CMB constraints on the reionization optical depth τ [25]
$$\tau = 0.0544 \pm 0.0073 \tag{60}$$

- the T_{cmb} constraint: $T_{cmb} = 2.7255 \pm 0.0006$ K [15],
  implies that the photon density is $\Omega_\gamma = 2.469 \times 10^{-5} h^{-2}$ and therefore we can reduce the radiation density $\Omega_r = \Omega_\gamma \left(1 + 0.2271 N_{eff}\right)$ and matter density to a function of just the parameter H_0

$$\Omega_r = 2.469 \times 10^{-5} h^{-2} \left(1 + 0.2271 \cdot 3.044\right) \tag{61}$$

$$\Omega_m = 1 - \Omega_r \tag{62}$$

Furthermore, the remaining two parameters of the IRPL model, i.e. the baryonic component of the matter density and the Hubble constant, must satisfy the following additional constraints:

1. The acoustic angular scale constraint: The acoustic oscillations in l seen in the CMB power spectra correspond to a sharply-defined acoustic angular scale on the sky, given by:

$$\frac{\pi}{\ell_a} = \theta_* = \frac{r_s^*}{d_M} \tag{63}$$

   where $r_s^* = r_s(z^*)$ is the comoving sound horizon at recombination quantifying the distance the photon-baryon perturbations can influence, $d_M(z^*)$ is the comoving angular diameter distance that maps this distance into an angle on the sky, and z^* depends on the ionization history and the atomic physics of recombination. It is possible to determine z^* by using the accurate recombination fitting formulae [19]. In this article, however, we have used the CAMB software [2], which provides very similar, but even more accurate results. *Planck* measures:

$$100\theta_* = 1.04109 \pm 0.00030 \quad (68\%, \text{TT,TE,EE+lowE}) \tag{64}$$

   a measurement with 0.03% precision.
   Because of its simple geometrical interpretation, θ_* is measured very robustly and almost independently of the cosmological model.
2. The BAO measurement constraint: The transverse baryon acoustic oscillation scale r_{drag}/d_M measured from galaxy surveys, where r_{drag} is the comoving sound horizon at the end of the baryonic-drag epoch, is the analogue of CMB acoustic angular scale.

   The BAO measurement constraint can be expressed as a approximate relation between $r_{drag} = r_s(z_{drag})$ and h, where z_{drag} is the redshift at the drag epoch, as:

$$\left(\frac{r_{drag} h}{\text{Mpc}}\right)\left(\frac{0.3}{\Omega_m}\right)^{0.4} = 101.056 \pm 0.036 \tag{65}$$

   for the ΛCDM $\mathcal{M}$etric [25]

$$\left(\frac{r_{drag} h}{\text{Mpc}}\right) = 101 \pm 1 \tag{66}$$

[2] CAMB is publicly available online at the following website: https://lambda.gsfc.nasa.gov/toolbox/tb_camb_form.cfm

for the $\mathcal{M}$etric of the present model (fig. 5).

3. "Late universe" H_0 measurements constraint: "Late universe" H_0 measurements using calibrated distance ladder techniques have converged on a value of approximately $H_0 \simeq 73.4$ km/s/Mpc. In particular, 73.4 ± 1.4 km/s/Mpc [27] from standard distance ladder, 73.3 ± 1.7 km/s/Mpc [38] from strong gravitational lensing effects on quasar systems.
4. the angular power spectrum of the CMB. At last, in addition to the constraints already expressed on the acoustic angular scale and on the scalar spectral index, the angular power spectrum of the CMB, within the assumptions underlying the standard model, provides precise measurements of the baryon density and dark matter density of the universe at recombination [18]. In particular, 2nd/1st peak ratio allows to determine the baryon density, one of the most robust and best-determined CMB outputs, since it controls the relative amplitudes of the alternating odd and even peaks, which correspond to modes undergoing maximal compression and rarefactions at the time of recombination.

   The [25], for the base-ΛCDM model from Planck CMB power spectra, in combination with CMB lensing reconstruction, finds, for TT,TE,EE+lowE+lensing 68% limits:

$$\omega_b = 0.02237 \pm 0.00015 \qquad (\omega_c = 0.1200 \pm 0.0012)$$

5. the growth of the cosmological perturbations: due to gravitational instability, cosmic structures have grown on the foundation of the first density fluctuations (59) that resulted from inflation. It is possible to follow the development of the so-called cosmological perturbations by looking at the large-scale structure of the Universe and how it has changed across the cosmic epochs. The most recent cosmic shear data release [32] from KiDS+VIKING-450 [31] and from both KiDS-1000 and DESY3 [33], confirms a tension with the Standard Model

$$S_8 = \sqrt{\frac{\Omega_m}{0.3}}\sigma_8 = 0.737^{+0.040}_{-0.036} \quad \text{from KiDS+VIKING-450.} \tag{67}$$

6. BBN predictions and primordial element abundances measurement constraint. In the present article we have used the version 2 of the software AlterBBN [3] suitably modified to adapt it to the different nuclear reaction rates of the present model which are half of the standard ones. Indeed, $\rho_b(z_{BBN}) = 0.5\,\rho_{0_b}$.
7. the acceleration in the expansion of the universe determined by comparing the brightness or faintness of distant supernovae relative to the empty Universe model [28].

[3] AlterBBN can be downloaded from the website: https://alterbbn.hepforge.org/. It is an open public code for the calculation of the abundance of the elements from Big-Bang nucleosynthesis in alternative cosmological scenarios, in a fast and reliable way. For the purpose of the IRPL model, the *bbnrate.c* file was modified by adding the instruction " **f[ie]=0.5*f[ie]**;" at the end of the loop of the *rate_all* function in order to halve all the reaction rates.

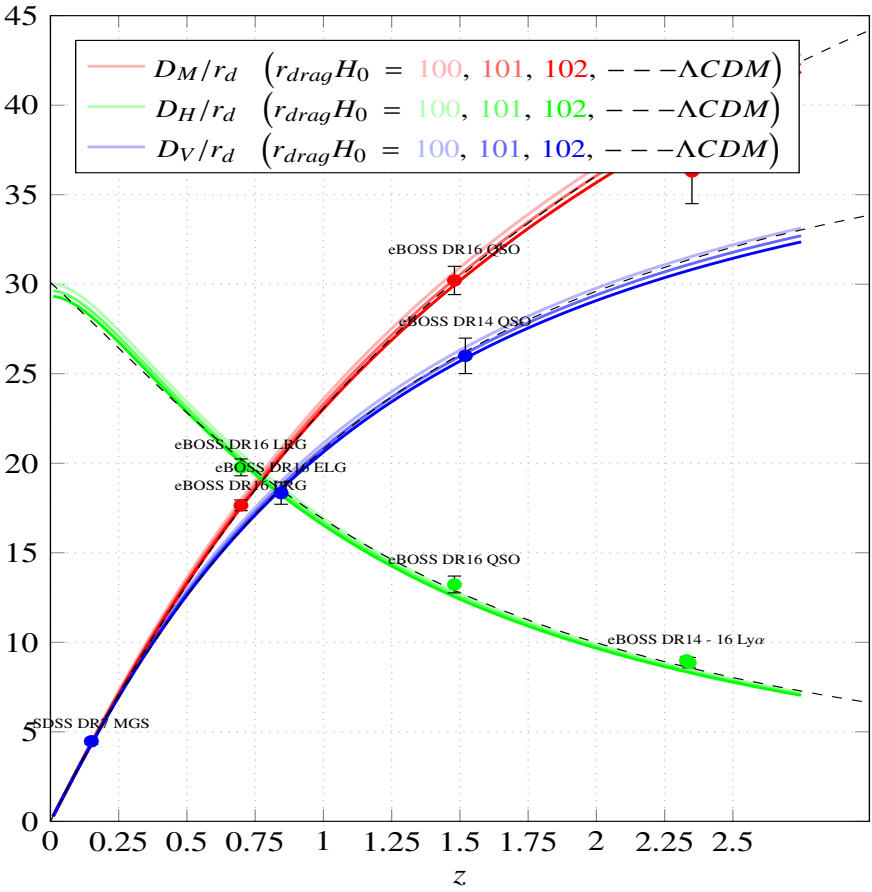

Fig. 5 BAO "Hubble diagram" : Black dashed lines represent the fiducial ΛCDM model, coloured solid lines represent the fiducial IRPL model for $H_0 r_{drag} = 100, 101, 102$.

6 Testing the IRPL model

The z^* and z_{drag} depend on the ionization history taking into account the atomic physics of recombination at the last scattering and drag epochs respectively. Since it is important to achieve the highest level of accuracy, the CAMB software was used to determine z^* and z_{drag} (table A1), making sure to use the appropriate values of $\omega_b(z)$ and $\omega_c(z)$ present at the redshift of interest, instead of the fitting formulas [19]. For the same reason, the exact formula of the acoustic wave speed (54) was used, which also takes into account the pressure of baryonic matter, and not the approximate one, although the results differ by only a few units on the second decimal place.
Therefore, given the *IRPL* metric $\mathcal{M}_{IRPL}(h)$ and the acoustic sound speed formula $c_s(\omega_b)$, for each ω_b we look for the value of h which satisfies both of the following equations at the same time:

$$z^* = z^*_{Camb}\left(\omega_{bs}(z^*), \omega_{cs}(z^*)\right) \tag{68}$$

$$\frac{r_s(z^*)}{\theta_* = 0.0104109} = d_M(z^*) \tag{69}$$

As a result, reaching an approximation of at most a few units on the second decimal place, we find that the acoustic angular scale constraint is satisfied by the values of z and h in accordance with the following fitting formulas in the range $H_0 = 73.48 \pm 1.5$ and $\Omega_b h^2 = 0.02325 \pm 0.005$ ($N_{eff} = 3.044$) (fig. 7)

$$z^* = 1134.3 + (H_0 - 73.48)\,8.85 - 2000\left(\Omega_b h^2 - 0.02325\right) \pm 0.05 \tag{70}$$

$$H_0 = 73.48\left(\frac{\omega_{0_b}}{0.02325}\right)^{-0.0378} \pm 0.05 \quad Mpc^{-1}Km/sec \tag{71}$$

Likewise, taking into account the BAO measurements constraint:

$$z_{drag} = z_{drag_{Camb}}\left(\omega_{bs}(z_{drag}), \omega_{cs}(z_{drag})\right) \tag{72}$$

$$r_s(z_{drag})h \simeq 101 \pm 1 \tag{73}$$

we find the following additional limitations on the ω_{0_b} and H_0 parameters (table A1 and fig. (5, 9, 7):

$$r_{drag} \simeq \frac{101.052}{h}\left(\frac{\omega_{b_0}}{0.02325}\right)^{-0.0675} \pm 0.05 \quad \text{Mpc} \tag{74}$$

$$\omega_{b_0} = 0.02335 \pm 0.00335 \qquad H_0 = 73.5 \pm 0.4 \tag{75}$$

Remarkably, throughout the aforementioned wide range $\Omega_b h^2 = 0.02325 \pm 0.005$, the IRPL metric together with the acoustic sound speed, having as the only free parameter to be able to vary the Hubble constant H_0, satisfy simultaneously all the first three aforementioned constraints. In particular, they satisfy the (68) and (69) with an accuracy of at most a few units on the second decimal place.

Regarding the baryon density limitation based on CMB constraints, found for the ΛCDM model, the same result can be applied equally well to the IRPL model taking into account the appropriate causal region:

$$\omega_b(\theta^*) = \frac{\Omega_{b_0}}{(1 + \sin\theta^* + \theta^*\cos\theta^*)^2} = 0.02237 \pm 0.00015 \tag{76}$$

which gives $\Omega_{b_0} = 0.023311 \pm 0.000156$. Therefore

$$z^*(\Omega_{b_0}) = 1134.22 \pm 0.6 \qquad H_0(\Omega_{b_0}) = 73.47 \pm 0.03 \tag{77}$$

$$\omega_c(\gamma^*) = \frac{\omega_{c_0}}{(1 + \sin\gamma^* + \gamma^*\cos\gamma^*)^2} = 0.1213 \pm 0.0001 \tag{78}$$

Table 1 Primordial abundances of elements in the big-bang nucleosynthesis (BBN)
For the measured values see: (a) Aver et al. [4], (b) Cooke et al. [8] , (c) Bania et al. [5], (d) Sbordone et al. [30]
For the ΛCDM calculated values see: Pitrou et al. [24]
The IRPL calculated values were produced by the software AlterBBN halving all the rates of nuclear reactions and with $\eta = 6.38158 \times 10^{-10}$, $\tau_n = 879.4$, $N_{eff} = 3.044$

	Yp (10^{-01})	D/H (10^{-05})	^{3}He/H (10^{-05})	^{7}Li/H (10^{-10})
Observations:	2.453 ± 0.034 (a)	2.527 ± 0.030 (b)	1.1 ± 0.2 (c)	$1.58\ ^{+0.35}_{-0.28}$ (d)
ΛCDM ($\eta_{10} = 6.13792$):	2.4721 ± 0.00014	2.439 ± 0.037	1.039 ± 0.014	**5.464 ± 0.220**
IRPL ($\eta_{10} = 6.38158$):	2.447 ± 0.0032	**6.528 ± 0.063**	1.502 ± 0.016	1.568 ± 0.11

At last, it is possible to use CAMB software to get a first approximation of the temperature variations of the CMB and of the power spectrum of matter density fluctuations within the IRPL model. About temperature variations of the CMB, we can see the Camb output (see fig. 8 and table A2), where the abscissas are slightly enlarged due to the slower velocity of c_s in the ΛCDM model. It is reasonable to adopt the same causal region, i.e. the same cosmic parameters ($H_0 = 73.48, \Omega_b(\theta^*)h^2 = 0.02237, \Omega_c(\gamma^*)h^2 = 0.1213$), also to get a first approximation of the matter power spectrum. Camb gives $\sigma_8 = 0.8123$. Since $\Omega_m(z_{eq}) = 0.24054 \pm 6 \times 10^{-6}$, it follows $S_8 = \sqrt{\Omega_m(z_{eq})/0.3}\sigma_8 = 0.727 \pm 0.007$ in good agreement with KiDS+VIKING-450.

At last, compared to the ΛCDM model, the IRPL model solves the Hubble Tension (at 5σ) while having one less parameter to play with.

BBN is one of the pillars of ΛCDM cosmology. The predictions of the standard BBN theory rest on balance between expansion rate and on the astrophysical nuclear reaction rates and on three additional parameters, the number of light neutrino flavours (N_ν), the neutron lifetime (τ_n) and the baryon-to-photon ratio ($\eta = n_B/n_\gamma$) in the universe [9]. Compared to the ΛCDM model, with the same baryon-to-photon ratio ($\eta = n_B/n_\gamma$), in the IRPL model the element densities during the BBN are half, and therefore the rates of astrophysical nuclear reactions during the BBN must be halved in the same way.
Table (1) and fig. (6) compare the values calculated by the IRPL model with those of the ΛCDM model and with those measured. Both the abundances of lithium-7 and helium-4 are congruent with the measured values. About the primordial ^{3}He abundance, at present there are no reliable measurements Cooke et al. [8], since ^{3}He can be both created and destroyed in stars. At last, IRPL BBN (table 1, table 3 and fig. 6) solves the lithium problem but, in its place, raises a deuterium problem.

About the acceleration in the expansion of the universe, from the (51) it follows that the accelerated expansion of the universe (fig. 2) has begun since $z \simeq 0.5099$ when the universe was 7.996 billion years old, roughly almost 5 billion years ago, since the age of the universe is 12.826 billion years.

7 Galaxy rotation curves

Nature reverses the lengths in the transition from the inside to the outside.

Table 2 Parameters for the base ΛCDM and IRPL models compared
Comparison between IRPL parameters and Parameter 68% intervals for the base-ΛCDM model from Planck CMB power spectra, in combination with CMB lensing reconstruction [25].

Parameter	ΛCDM TT,TE,EE+LowE+lensing 68% limits	IRPL	IRPL special cases
ω_{0_b}	0.02237 ± 0.00015	0.023163 ± 0.00035	$\omega_b(\theta^*) = 0.02231 \pm 0.00033$
ω_{0_c}	0.1200 ± 0.0012	0.5166 ± 0.001	$\omega_c(z^*) = 0.1212 \pm 0.0002$
$100\theta_{MC}$	1.04092 ± 0.00031	idem	
τ	0.0544 ± 0.0073	idem	
$ln\left(10^{10}A_s\right)$	3.044 ± 0.014	idem	
n_s	0.9649 ± 0.0042	idem	
$H_0[kms^{-1}Mpc^{-1}]$	67.36 ± 0.54	73.48 ± 0.04	
Ω_Λ	0.6847 ± 0.0073		
Ω_m	0.3153 ± 0.0073	$0.999923 \pm 8 \times 10^{-8}$	$\Omega_m(z_{eq}) = 0.240540 \pm 6 \times 10^{-6}$
Age[Gyr]	13.797 ± 0.023	12.818 ± 0.07	
z^*	1089.92 ± 0.25	1134.3 ± 0.05	
$r^*[Mpc]$	144.43 ± 0.26	129.44 ± 0.05	
$100\theta^*$	1.04110 ± 0.00031	1.04101	
z_{drag}	1059.94 ± 0.30	1036.45 ± 0.7	
$r_{drag}[Mpc]$	147.09 ± 0.26	137.53 ± 0.7	
z_{eq}	3402 ± 26	3108.37 ± 4.3	
σ_8	0.8111 ± 0.0060	0.8123 ± 0.007	
S_8	0.832 ± 0.013	0.727 ± 0.007	

In the physics of the universe, inside the Radius of the universe, i.e. in cosmology, where $r \leq R_0 = R_\Omega$ and $\tau^\diamond = R_0 = R_\Omega$, we have:

$$\frac{1}{R_\Omega} = \frac{1}{R_{\Omega_r}} + \frac{1}{R_{\Omega_b}} + \frac{1}{R_{\Omega_c}} \qquad \equiv \qquad 1 = \Omega_r + \Omega_b + \Omega_c \tag{79}$$

and given the relationship between space and mass-energy (see eq. 39), it is possible to break down the elements of the metric according to the type of energy:

$$\frac{1}{r_{max}^2} = \frac{1}{R_0 R_\Omega} = \frac{\Omega_r}{R_0^2} + \frac{\Omega_b}{R_0^2} + \frac{\Omega_c}{R_0^2} \tag{80}$$

$$\frac{1}{r^2} = \frac{1}{r_r^2} + \frac{1}{r_b^2} + \frac{1}{r_c^2} = \left(\frac{1}{R_0 R_{\Omega_r}} + \frac{1}{R_0 R_{\Omega_b}} + \frac{1}{R_0 R_{\Omega_c}}\right) \frac{1}{(\sin\gamma)^2} = \frac{\Omega_r + \Omega_b + \Omega_c}{r^2} \tag{81}$$

$$\frac{1}{\mathrm{d}d_M^2(z)} = \frac{1}{\mathrm{d}d_{M_r}^2(z)} + \frac{1}{\mathrm{d}d_{M_b}^2(z)} + \frac{1}{\mathrm{d}d_{M_c}^2(z)} = \frac{H^2(z)}{c^2 \mathrm{d}z^2} = \frac{H_r^2(z) + H_b^2(z) + H_c^2(z)}{c^2 \mathrm{d}z^2} \tag{82}$$

On the other hand, in the physics of galaxies outside the radius of galaxies, the gravitational radius of a galaxy, neglecting the radiation, and since, from the (eq. 39), $R_c \simeq r^2/R_0$, is :

$$R = \Omega_b R + \Omega_r R + \Omega_c R = R_b + R_c + R_r \simeq R_b + r^2/R_0 + 0 \tag{83}$$

Similarly to what has been done in cosmology, it is possible to decompose the distance according to the type of energy and in particular it is convenient to impose that the curvature radius, equal to the inverse of the acceleration, is the same for all the components everywhere, namely:

$$A_x = \frac{R_x}{r_x^2} = A = \frac{R}{r^2} = \frac{1}{\tau^\diamond} \qquad (R_{galaxy} \leq \tau^\diamond \leq R_0) \tag{84}$$

which is the dual of the (2) for $r \geq R$. This condition is satisfied by $r_x = \sqrt{\Omega_x}\, r$ or, equivalently:

$$r^2 = r_b^2 + r_r^2 + r_c^2 = \Omega_b\, r^2 + \Omega_r\, r^2 + \Omega_c\, r^2 \tag{85}$$

which is the dual of the (81) for $r \geq R$ (note that, since $R \simeq R_b + R_c$, we have $A_{gravitational} \simeq \frac{R_b}{r^2} + \frac{1}{R_0}$).

If we set

$$A_{centrifugal} = \frac{v_{centrifugal}^2}{r_b} \tag{86}$$

since in the orbital motion $A_{gravitational} = A_{centrifugal}$, it follows:

$$v_{centrifugal} = \sqrt{V_b} = \sqrt[4]{\frac{R}{r^2} R_b} = \sqrt[4]{\frac{R_b^2}{r^2} + \frac{R_b}{R_0}} \tag{87}$$

and the limits

$$r_{b_\infty} = \lim_{r \to R_0} \sqrt{\frac{R_b}{R}}\, r = \sqrt{R_b R_0} \tag{88}$$

$$v_\infty = \lim_{r \to R_0} \sqrt[4]{\frac{R_b^2}{r^2} + \frac{R_b}{R_0}} = \sqrt[4]{\frac{R_b}{R_0}} \tag{89}$$

On circular orbit, where $R_0 = 2\pi c H_0^{-1}$, we find (see fig. 10), with the same mass distribution, that the predictions for the galaxy rotation curves from present work (eq. 87) and MSTG and Milgrom's Mond agree remarkably for all of the 101 galaxies reported in [7]. It is relevant that the Newton velocity, once replaced the total distance r with the distance r_b, is consistent with the experimented values everywhere (see fig. 10).

On radial orbits, stars plunging in and out of the galactic center, $R_0 = cH_0^{-1}$, as in motion of satellite galaxies around normal galaxies at distances 50-500 kpc [20], the rotation curves are considerably affected by the radial component of the motion which gradually decreases as moving away from the host galaxy. The maximum speed $v_\infty = \sqrt[4]{\frac{R_b}{R_0}}$ consequently decreases as $\sqrt[-4]{2\pi}$ as the initial radial speed turns into tangential speed moving away from the host galaxy consistently with the experimental results.

Very interesting is the determination of the barycentre. From

$$\sum_{i=1}^{n} (M_{b_i} \ddot{r}_{b_i}) = M_{b_{Tot}} \ddot{r}_b \tag{90}$$

we have the barycentre coordinates:

$$r_b = \sum_{i=1}^{n} \frac{M_{b_i}}{M_{b_{Tot}}} r_{b_i} = \sum_{i=1}^{n} \frac{M_{b_i}}{M_{b_{Tot}}} \sqrt{\frac{M_{b_i}}{M_{b_i} + \frac{r_{cdm_i}^2}{R_\omega}}} r_i = \sum_{i=1}^{n} \frac{M_{b_i}}{M_{b_{Tot}}} \frac{r_{b_{max_i}}}{\sqrt{r_{b_{max_i}}^2 + r_{cdm_i}^2}} r_i \tag{91}$$

A huge quantity of mass, fractioned in little parts far away, is negligible with respect to a much smaller quantity of mass concentrated in bigger parts.

At last, the presumed direct proof of Dark matter [*Clowe et al. 2006*], given by the recent observed collision of two clusters of galaxies ("bullet cluster" 1E0657-56), where it is shown that the sources of gravity in the cluster are not located where the ordinary matter is located, can be explained by the correct determination of the barycentre. The (91), indeed, predicts the irrelevance of the huge quantity of dominant tiny matter component, that is the X-ray plasma clouds, with respect to the very more large masses constituted by the galaxy clusters.

Likewise, the (91) can explain the recent observation of already-evolved ultra-distant galaxies at the early stage in cosmic history ($z > 11$ see [40]). Indeed, the special weight that, in determining the center of gravity, acquire in the (91) concentrations of baryonic matter higher than the average, favours the growth of the agglomerations in a decidedly greater way than what is supposed by current physics. This provides an explanation of how it was possible to go from a Universe that was born almost perfectly uniform, with the densest regions just a few parts in 100,000 denser than average, to one that's rich in evolved, massive galaxies in only a few hundred million years.

At last, the part of relationship $R_{part} : R_{whole} = R_{whole} : R_\omega$ requires that every relation finds its place inside an individual more complex of which it is a part of, providing all the mirroring universe scale: stars, galaxies, clusters and so on.

8 Conclusion

It is worthy of attention that the IRPL's BBN theory, which predicts the halving of the rates of primordial nuclear reactions in comparison to the standard model theory, is supported by measurements of primordial element abundances at least as much as the latter, while predicting very different results. Remarkably, it solves the primordial lithium problem, although it introduces a deuterium problem. It is worthy of attention that the IRPL model meets the cosmological constraints derived from the CMB and BAO, as well as the acceleration of the universe's expansion, while relying on one fewer parameter in an equally satisfying manner as the ΛCDM model. Mostly, it solves the tension between the direct and the inverse cosmic distance ladder and the growth or S_8 tension and provides an explanation to the recent observation of

already-evolved ultra-distant galaxies at the early stage in cosmic history. Finally, the model is successful on both large and small scales by resolving the issues associated with rotation in the interior sections of spiral galaxies using the same hypothesis that underpins the IRPL model, with findings comparable to those of the Mond theory.

About the matter density, it does not violate the cosmological principle of the homogeneity of space because it applies equally in every place. Furthermore, its dependency on distance indicates that the CDM's dimensions match to the quantum of space, implying that it will never be observed directly. To put it another way, if ordinary matter is matter in act and all interactions mediated by bosons occur in the act, CDM is matter in potency and gravity occurs in the potency.

The reciprocal rotation angle γ, which relies on the Radii involved, governs an inertial system as well as a force field at any given time. The radius between an emitter-receiver pair increases throughout the universe, similar to an inertial frame, as $R = V^{\diamond} r^{\diamond} = V^{\diamond 2} \tau$. Contrary to an inertial frame, however, for the universe $\tau = \tau_{max} = R_{\omega}$, where R_{ω} denotes the universe's conservative total energy. This energy, which has existed since the Big Bang, creates the dynamics of the universe's expansion as stated by Friedmann's equations, which now comes to a halt shortly before turning about.

However, since all observable physics comes from the path of light, the evolution of a body along time must also be understood as a path of light. Light always has a starting point and a destination point, it always moves between a sender and a receiver. In summary, the following points apply to the universe:

- the universe has a curvature radius R_0 equal to its gravitational radius R_{Ω}
- the horizon of the present in act has constant surface gravity equal to H_0
- the change of energy ($r_s = r^2/R_0$ from hypothesis 2) is related to change of area A, angular momentum J, and electric charge Q by

$$dE = \frac{\kappa}{8\pi} dA + \Omega\, dJ + \Phi\, dQ \tag{92}$$

for $dJ = dQ = 0$, being the surface gravity $\kappa = 1/r$ and where A is the horizon area.

Finally, these evidences point to a different solution to the causal horizon problem. In truth, the ad hoc inflation hypothesis might be replaced with the more natural and general hypothesis:

Hypothesis 3 *The universe is a white/black hole with constant Schwarzschild Radius* $R_{\Omega} \equiv c/H_0$ *where the big bang/big crunch is not an event of the past but a continuous feedback process, always in progress, typical of all black holes. It follows that the surface of the present in act* ($\gamma = 0$)*, as well as the big bang in act* ($\gamma \pm \pi/2$)*, are the frontiers where the approaching future becomes present and is converted in the past that moves away and vice versa. This cyclicity, however, does not rule out the possibility that the cosmos, like a black hole, has a beginning and an end.*

The universe is a circular wheel formed by the continual journey of light that closes on itself. The Big Bang is its center and equivalently the point of the wheel at $+\pi/2$ with regard to the point of the wheel which represents the here and now. The Big Crunch is its anticenter and equivalently the point of the wheel at $-\pi/2$. The sine represents the amount of time since the Big Bang, while the cosine represents the distance. Each point of the wheel is the here and now in which light passes from being received to being sent.
In other words, the internal volume of the sphere is the seat of potency, whereas the surface is the place of the present in act where the temporal axis of each individual emerges radially dividing the surface of the black hole into its own receiving hemisphere ($0 \geq \gamma \leq \pi/2$), populated by all other individuals in the act of giving as matter, where the arrow of time is positive and entropy increases, and in its opposite giving hemisphere ($\pi/2 \geq \gamma \leq \pi$), populated by individuals in the act of receiving as antimatter, where the arrow of time is negative and entropy decreases.

In other words, for each individual, the present, which comes from the continuous Big Bang (as source) as an approaching future (matter and increasing entropy), as soon as it surfaces, it submerges as past (antimatter and decreasing entropy) that move away to go towards the continuous Big Crunch (as well), and in this descent informs of itself the future that ascend in the opposite direction. The past that is moving away is also the future that is approaching, and it is the possibility of the present. The present is the realization of a possible history of the past, among the totality of physically possible histories in accordance with quantum mechanics.
The mechanism that places the same initial conditions everywhere, therefore, is not to be found in a causal contact occurred in the past of a linear time, but in the dialogue, with a period P_ω equal to the apparent age of the universe, between the big bang and the present, in a cyclical time: each time, the new present in act is the result of the big bang that took place P_ω years before and is the foundation of the big bang that will take place P_ω years later.
This hypothesis, compared to the correspondent of standard cosmology, radically changes the meaning but leaves the entire phenomenology and physics of the universe unchanged. If this hypothesis is correct, all the parameters of the universe are not contingent but intimately connected with the geometry of the universe.

The surface is the determined act, the interior is the power that explains it, the surface is electrical, the interior gravitational, the surface is the consciousness, the interior the soul. At last, a telescope is not a “time machine”, rather, it is a “power machine”.

References

[1] Addison G. E., Huang Y., Watts D. J., Bennett C. L., Halpern M., Hinshaw G., Weiland J. L., 2016, [ApJ] , 818,132

[2] Akita K., Yamaguchi M., 2020, [J. Cosmology Astropart. Phys.] , 2020,012

[3] Aubourg A., Balembois F., Georges P., 2014, [Laser Physics Letters], 11,048001

[4] Aver E., Berg D. A., Olive K. A., Pogge R. W., Salzer J. J., Skillman E. D., 2021, [J. Cosmology Astropart. Phys.] , 2021,027

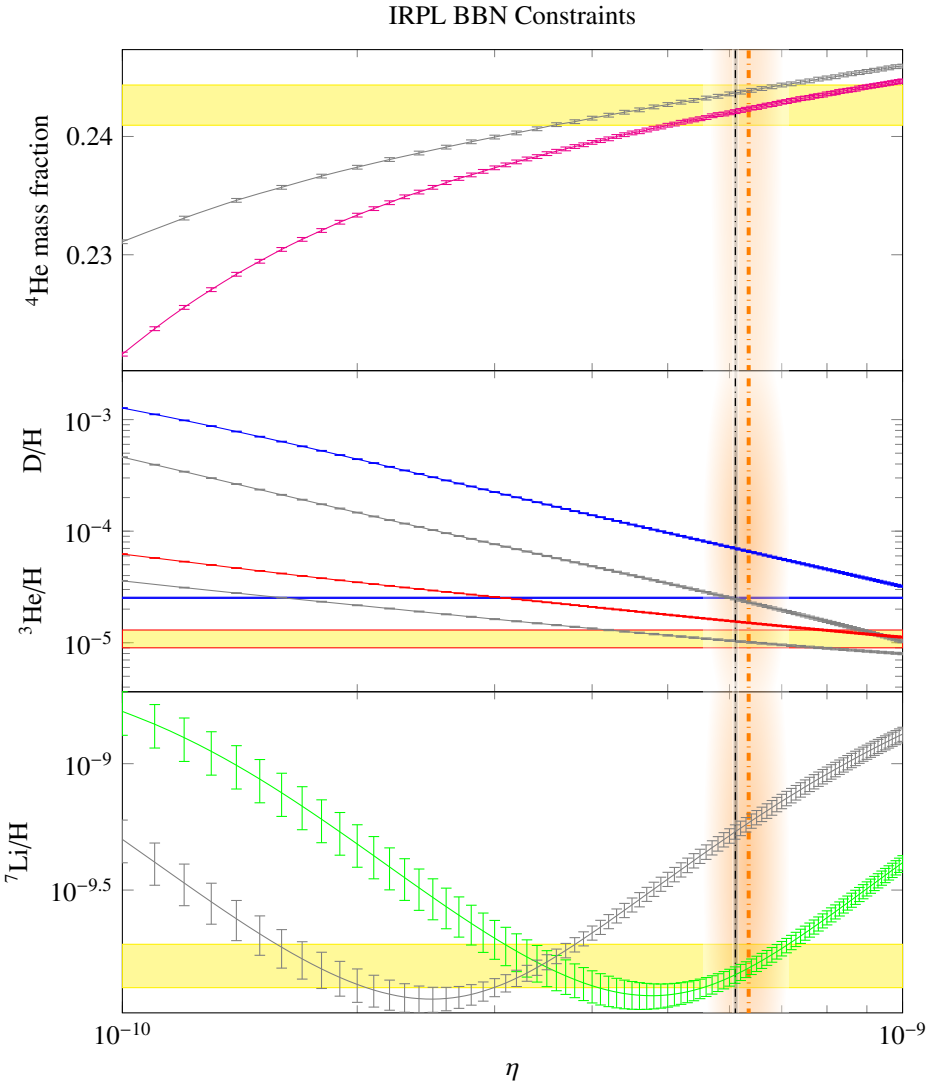

Fig. 6 Comparison between the primordial abundances expected for the light nuclei according to the ΛCDM model, grey lines, and the IRPL model, coloured lines. Yellow horizontal rectangles show range of the uncertainties in the primordial abundances measured values (see table 3). The orange vertical line indicates the value of $\eta = 6.35 \pm 0.8 \times 10^{-10}$ deduced in the present IRPL analysis, the grey one $\eta = 6.105 \pm 0.055 \times 10^{-10}$ for the ΛCDM model [23]. The values were calculated using the version 2 of *AlterBBN* software, an open public code for the calculation of the abundance of the elements from Big-Bang nucleosynthesis. For the purpose of the IRPL model, the *bbnrate.c* file was modified by adding the instruction " **f[ie]=0.5*f[ie];** " at the end of the loop of the *rate all* function in order to halve all the reaction rates.

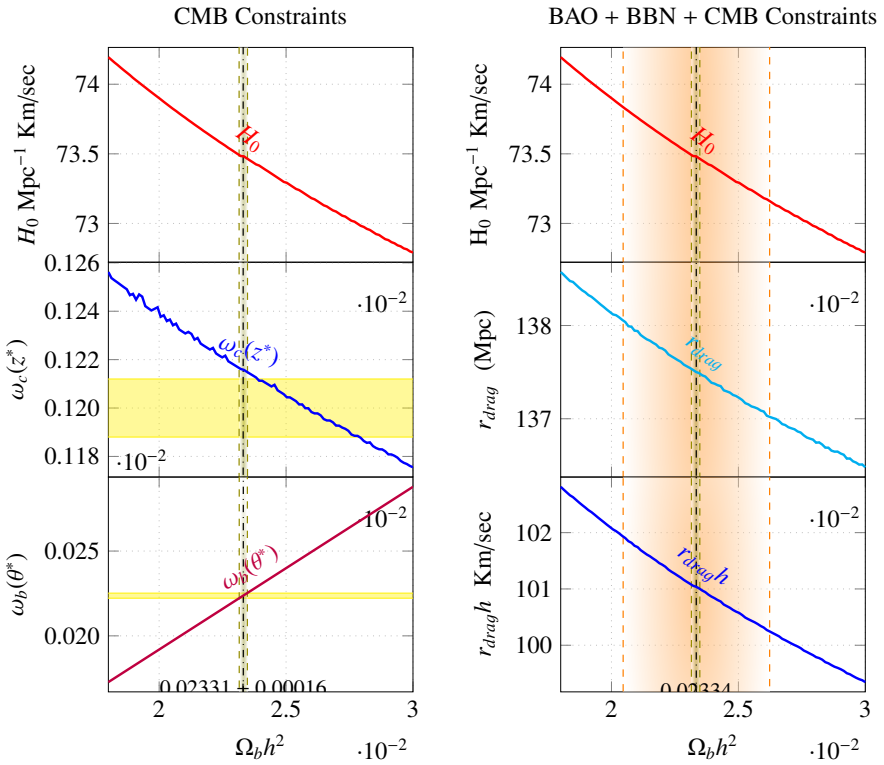

Fig. 7 On the left panel the CMB constraints on the Hubble constant. On the right, the superimposition of all the constraints on the parameters of the IRPL model.

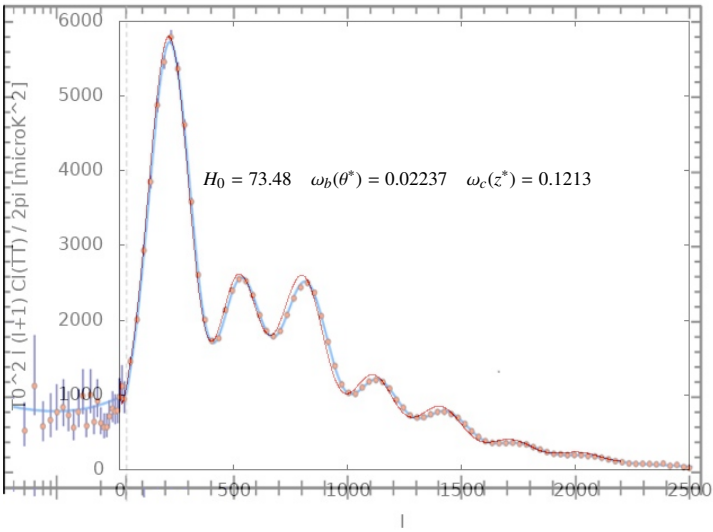

Fig. 8 The CMB temperature (E-mode polarization), output of CAMB with $\omega_c(z^*) = 0.1213$, $\omega_b(\theta^*) = 0.02237$ (which corresponds to $\omega_{0_b} = 0.02331$).

Table 3 Primordial abundances of elements in the big-bang nucleosynthesis (BBN)

	Yp (10^{-01})	D/H (10^{-05})	^{3}He/H (10^{-05})	^{7}Li/H (10^{-10})
measured values:	2.453 ± 0.034 (a)	2.527 ± 0.030 (b)	1.1 ± 0.2 (c)	$1.58^{+0.35}_{-0.28}$ (d)
...	...	...	...	...
calculated values (η_{10} = 5.5):	2.430 ± 0.0032	8.283 ± 0.074	1.666 ± 0.016	1.290 ± 0.11
calculated values (η_{10} = 5.6):	2.432 ± 0.0032	8.046 ± 0.072	1.645 ± 0.016	1.312 ± 0.11
calculated values (η_{10} = 5.7):	2.435 ± 0.0032	7.821 ± 0.071	1.624 ± 0.016	1.337 ± 0.11
calculated values (η_{10} = 5.8):	2.437 ± 0.0032	7.606 ± 0.069	1.605 ± 0.016	1.365 ± 0.11
calculated values (η_{10} = 5.9):	2.438 ± 0.0032	7.400 ± 0.068	1.586 ± 0.016	1.395 ± 0.11
calculated values (η_{10} = 6.0):	2.440 ± 0.0032	7.204 ± 0.067	1.567 ± 0.016	1.427 ± 0.11
calculated values (η_{10} = 6.1):	2.442 ± 0.0032	7.015 ± 0.065	1.549 ± 0.016	1.461 ± 0.11
calculated values (η_{10} = 6.2):	2.444 ± 0.0032	6.836 ± 0.065	1.532 ± 0.016	1.497 ± 0.11
calculated values (η_{10} = 6.3):	2.446 ± 0.0032	6.663 ± 0.063	1.515 ± 0.016	1.535 ± 0.11
calculated values (η_{10} = 6.36515):	2.447 ± 0.0032	6.555 ± 0.063	1.504 ± 0.016	1.562 ± 0.11
calculated values (η_{10} = 6.4):	2.448 ± 0.0032	6.497 ± 0.062	1.499 ± 0.016	1.576 ± 0.11
calculated values (η_{10} = 6.5):	2.449 ± 0.0032	6.339 ± 0.061	1.483 ± 0.016	1.618 ± 0.11
calculated values (η_{10} = 6.6):	2.451 ± 0.0032	6.186 ± 0.060	1.468 ± 0.016	1.662 ± 0.11
calculated values (η_{10} = 6.7):	2.453 ± 0.0032	6.040 ± 0.060	1.453 ± 0.016	1.708 ± 0.11
calculated values (η_{10} = 6.8):	2.454 ± 0.0032	5.899 ± 0.059	1.438 ± 0.016	1.756 ± 0.12
calculated values (η_{10} = 6.9):	2.456 ± 0.0032	5.763 ± 0.058	1.424 ± 0.016	1.806 ± 0.12
calculated values (η_{10} = 7.0):	2.458 ± 0.0032	5.633 ± 0.056	1.410 ± 0.016	1.857 ± 0.12
calculated values (η_{10} = 7.1):	2.459 ± 0.0032	5.507 ± 0.056	1.397 ± 0.016	1.910 ± 0.12
calculated values (η_{10} = 7.2):	2.461 ± 0.0032	5.386 ± 0.055	1.383 ± 0.016	1.965 ± 0.13
...	...	...	...	...

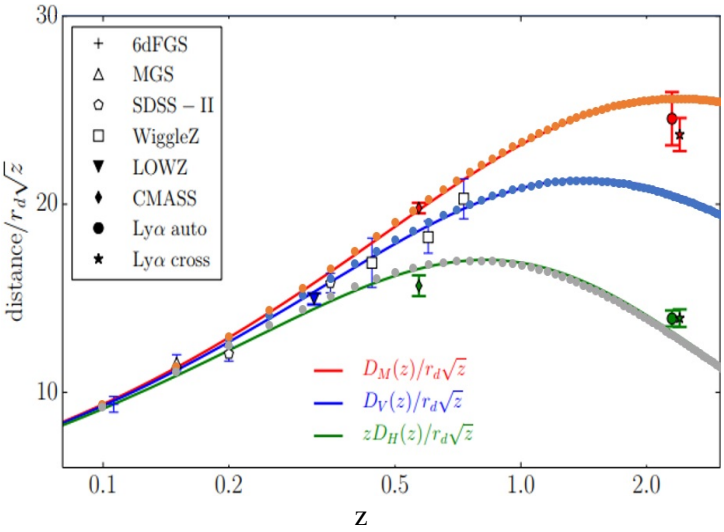

Fig. 9 The BAO "Hubble diagram" [from 3]. Blue, red, and green points show BAO measurements of d_V/r_d, d_M/r_d, and zd_H/r_d, respectively, from the sources indicated in the legend. The scaling by $\sqrt{z}$ is arbitrary, chosen to compress the dynamic range sufficiently to make error bars visible on the plot. These can be compared to the correspondingly colored lines, which represents predictions of the fiducial Planck ΛCDM model (with $m = 0.3183$, $h = 0.6704$) and the prediction of the IRPL model (dotted line) when $r_{s_{drag}} = 101.0/h$ Mpc.

[5] Bania T. M., Rood R. T., Balser D. S., 2002, [Nature], 415,54

[6] Bennett J. J., Buldgen G., Drewes M., Wong Y. Y. Y., 2020, [J. Cosmology Astropart. Phys.] , 2020,003

[7] Brownstein J. R., Moffat J. W., 2006, [ApJ] , 636,721

[8] Cooke R. J., Pettini M., Steidel C. C., 2018, [ApJ], 855,102

[9] Copi C. J., Schramm D. N., Turner M. S., 1995, [Science], 267,192

[10] Di Valentino E., et al., 2021, [Classical and Quantum Gravity], 38,153001

[11] Einstein A., 1905, [Annalen der Physik], 322,891

[12] Einstein A., 1923, The Meaning of Relativity, 1 edn. Princeton University Press, Princeton, NewJersey

[13] Escudero Abenza M., 2020, [J. Cosmology Astropart. Phys.] , 2020,048

[14] Feynman R. P., 1985, QED: The Strange Theory of Light and Matter, 1 edn. Princeton University Press, Princeton, NewJersey

[15] Fixsen D. J., 2009, [ApJ], 707,916

[16] Froustey J., Pitrou C., Volpe M. C., 2020, [J. Cosmology Astropart. Phys.], 2020,015

[17] Grohs E., Fuller G. M., 2017, [Nuclear Physics B], 923,222

[18] Hu W., Dodelson S., 2002, [ARA&A], 40,171

[19] Hu W., Sugiyama N., 1996, [ApJ], 471,542

[20] Klypin A., Prada F., 2009, [ApJ], 690,1488

[21] Landau L. D., Lifshitz E. M., 1971, The Classical Theory of Fields, 3 edn. Pergamon Press Ltd., Headington Hill Hall, Oxford

[22] Mangano G., Miele G., Pastor S., Pinto T., Pisanti O., Serpico P. D., 2005, [Nuclear Physics B], 729,221

[23] Mindari W., Sasongko P. E., Kusuma Z., Syekhfani Aini N., 2018, in The 9th International Conference on Global ReSource Conservation (ICGRC) and Aji from Ritsumeikan University. p. 030001,

[24] Pitrou C., Coc A., Uzan J.-P., Vangioni E., 2021, [MNRAS], 502,2474

[25] Planck Collaboration et al., 2020, [A&A], 641,A6

[26] Pettini M., "Introduction to Cosmology", Lecture 2

[27] Reid M. J., Pesce D. W., Riess A. G., 2019, [ApJ], 886,L27

[28] Riess A. G., et al., 1998, [AJ] , 116,1009

[29] Riess A. G., et al., 2021, arXiv e-prints, arXiv:2112.04510

[30] Sbordone L., et al., 2010, [A&A], 522,A26

[31] Hildebrandt, H., Köhlinger, F., van den Busch, J. L., et al. [A&A] 2020,633,A69

[32] L. Perivolaropoulos and F. Skara, arXiv:2105.05208[astro-ph.CO].

[33] Asgari, M.; Lin, C.A.; Joachimi, B.; Giblin, B.; Heymans, C.; Hildebrandt, H.; Kannawadi, A.; Stölzner, B.; Tröster, T.; van den Busch, J.L.; et al.[A&A] 2021,645,A104

[34] Leonard Susskind, "The World as a hologram," J. Math. Phys. 36, 6377–6396 (1995), arXiv:hep-th/9409089

[35] Gerard 't Hooft, "Dimensional reduction in quantum gravity," in Salamfest 1993:0284-296 arXiv:gr-qc/9310026

[36] Bekenstein, Jacob D, Physical Review D, 49,4 1994 arXiv:gr-qc/9307035

[37] Vonlanthen M., Räsänen S., Durrer R., 2010, [J. Cosmology Astropart. Phys.], 2010,023

[38] Wong K. C., et al., 2020, Monthly Notices of the Royal Astronomical Society, 498, 1420

[39] de Salas P. F., Pastor S., 2016, [J. Cosmology Astropart. Phys.], 2016,051

[40] Haojing Yan et al 2023 ApJL 942 L9 10.3847/2041-8213/aca80c

[41] *Giordano Bruno: La Cena de le Ceneri, 1584*

[42] *Giordano Bruno: De la causa, principio et uno, 1584*

[43] *Giordano Bruno: De l'infinito, universo e mondi, 1584*

[44] *Peluso V. (2019) Intention Physics http://vixra.org/abs/1811.0391*

[45] *Peluso V. (2021) Intention not Theory: the Vertigo of Love http://vixra.org/abs/2003.0606*

[46] *Peluso V. (2021) The Geometry of the Discrete Act http://vixra.org/abs/2104.0097*

[47] *Peluso V. (2022) The Cosmology of the Instant Reconstruction of the Path of Light http://vixra.org/abs/2204.0175*

[48] *Peluso V. (2022) The Promised Science https://vixra.org/abs/2208.0071*

[49] *Peluso V. (2022) Individual, Time and Space https://vixra.org/abs/2209.0042*

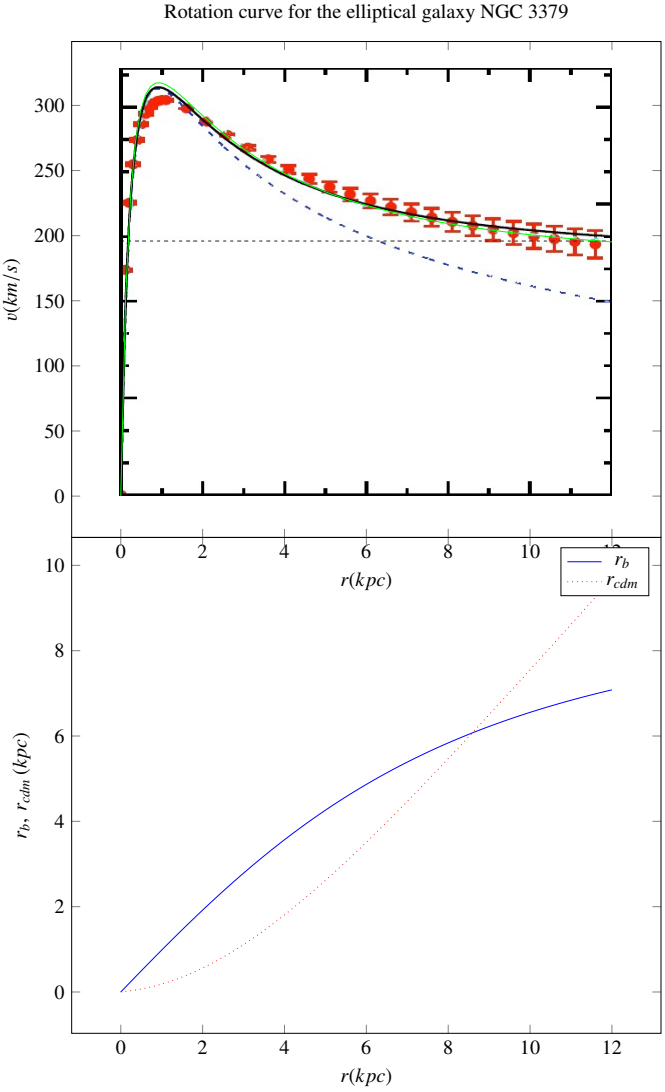

Fig. 10 On the top panel, the rotation curve for the elliptical galaxy NGC 3379. The red points (with error bars) are the observations. The solid green line is the rotation curve determined by the present work (eq. 87), the short dashed blue line is the Newtonian galaxy rotation curve. The same distribution of the galactic mass reported in [7] has been adopted, that is $M = 6.99\ 10^{10}\ M_{\odot}$, and a core radius $r_c = 0.45$ kpc and $\beta = 1$.
On the bottom panel, the trend of r_b and r_{cdm}. The rotation curve also corresponds to Newton's velocity once replaced the total distance r with the distance r_b.

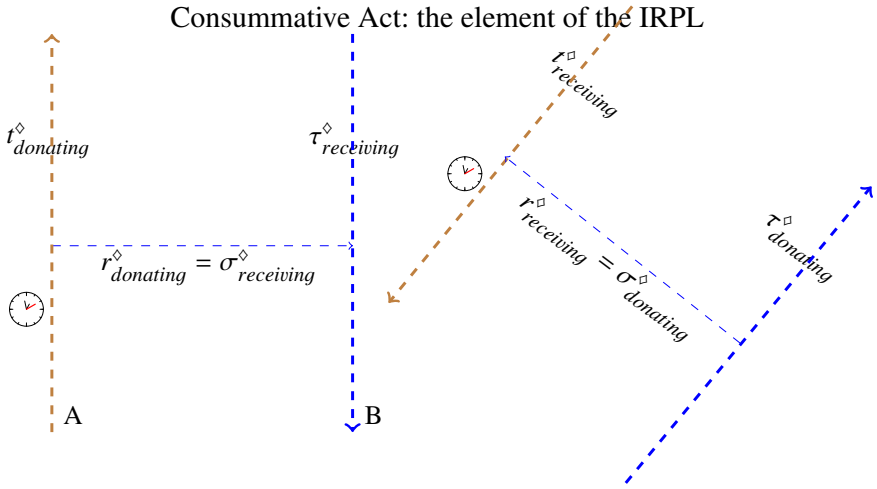

Fig. A1 Consummative Act (not the event) is the element of the IRPL: light does not have a speed, each segment of the path of light itself constitutes the space axis and determines the time axis, orthogonal to it, constituting the frames of the two individuals who oppose each other in the interaction. Consequently, for each individual, one frame corresponds to the act of giving and another frame corresponds to the act of receiving. The two frames are rotated to each other by a real γ angle. The determination of the γ angle is subject to the Uncertainty principle. Indeed, in a measurement, while the measuring instrument A is necessarily classic and therefore reflective, so we know $P^{\diamond} = t^{\diamond}_{A_i} - t^{\diamond}_{A_{i-1}}$, the measured B could be non-classic, therefore we would not know the proper time $t^{\diamond}_{B_i}$ and therefore we would not know $\cos\gamma^{\diamond} = \frac{t^{\diamond}_{B_i} - t^{\diamond}_{A_{i-1}}}{t^{\diamond}_{A_i} - t^{\diamond}_{B_i}}$ and vice-versa.

Appendix A The discrete one-dimensional geometry of the Act

Because the act is instantaneous, so is the radiant energy: the receiving side of one faces the parallel and opposite donor side of the other, and vice versa: in the act there are no distances or, more correctly, they are veiled and cannot be known, (see fig. A1), nor is the other's identity known.

Nonetheless, reflective individuals (classic objects) emerge through the superposition, layering, and nesting of countless elementary intentions, interacting with one another via reflective intentions. Both in the period of potency and in the instant of the act, individuals are in relation to each other. This relationship is the Reflection in the instant of the Act, it is the Mirroring in the period of Power. Mirroring is the foundation of reflection and this is the foundation of knowledge. Now, reflection is the unveiling of what is veiled in power. Mirroring does in potency what reflection does in the act. Mirroring and reflection are dual, one is the form (the universal) and the other is its fulfilment (an instance).

What matures in the potency, and is still veiled in every elementary act, is finally revealed in the reflective phenomenon that appears taking place in the present instant. The reflection appears as an image and the image emerges from the organization, i.e spatial arrangement, of the other intentions in the background. Reflection is the image

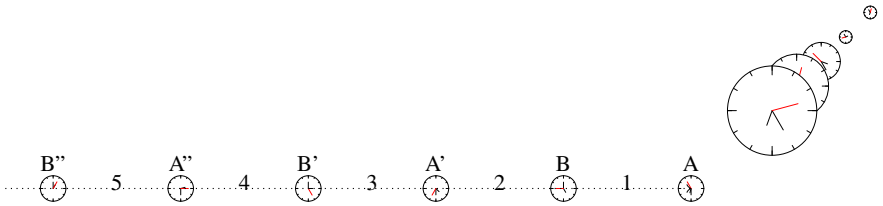

Fig. A2 Recursive mirroring: two mirrors facing each other are reflected recursively. If there is a clock on each of them, in the reflected image present in every instant it is possible to reconstruct distances historically and therefore the velocities and accelerations over time, as far as the reflection allows.

that emerges from the enormous number of underlying consummative acts, where each of these acts corresponds to a pixel. When, in the statistics of large numbers, the randomness due to the freedom is cancelled out, the phenomenon becomes deterministic and its rule is revealed by the image, since it is an epiphenomenon which carries epi-knowledge, such as the number of elapsed cycles marked by a counter. Memory, knowledge, logic, evolution, mechanisms, particles, theories, are all reflective.

Every reflecting individual in the intention is both a mirror and a wristwatch: a mirror in the period of potency, and a wristwatch in the historical reconstruction that occurs in the instant of the present in action. The mirrored world in the period of potency leaves the place to the historically reconstructed metric world of the instantaneous act. The instant, which is not time and has no movement, has instead in itself the representation of the movement that unfolds as space and time of the MEMORY.

A.1 The scheme underlying the mirroring

The IRPL (Instant Reconstruction of the Path of Light) or (Intention Relationship's PL) is only and not other than the reconstruction, starting from the present instant, of the path of the intermediaries of the interaction (i.e. the bosons) that takes place between two individuals in relationship. This is the same path as the light between two mirroring individuals: each one reflects and is reflected by the other recursively.

In fact, if we place a clock on each of the two individuals involved in the interaction (see fig. A2), we can historically reconstruct distances and time intervals from the sequence of times that appears in the mirror image. If we denote by $s_n^\diamond = t_n^\diamond - t_{n-1}^\diamond$ the distance between the two individuals at time t_n, we discover (see fig. A3) that the historical reconstruction of the distance series forms a geometric progression

$$t^\diamond = s_0^\diamond + s_1^\diamond + s_2^\diamond + s_3^\diamond + \ldots = s_0^\diamond \left(1 + K^\diamond + K^{\diamond 2} + K^{\diamond 3} + \ldots\right) = \frac{s_0^\diamond}{1 - K^\diamond}$$

where $s_0^\diamond$ is the scale factor and $k = \cos^\diamond \gamma$ is the common ratio. Therefore

$$\Delta\lambda^\diamond = t^\diamond - t_{-1}^\diamond = s_0^\diamond \quad \text{and} \quad V^\diamond = \frac{\Delta\lambda^\diamond}{t^\diamond} = \frac{\overline{AB}}{\overline{0A}} = 1 - K^\diamond$$

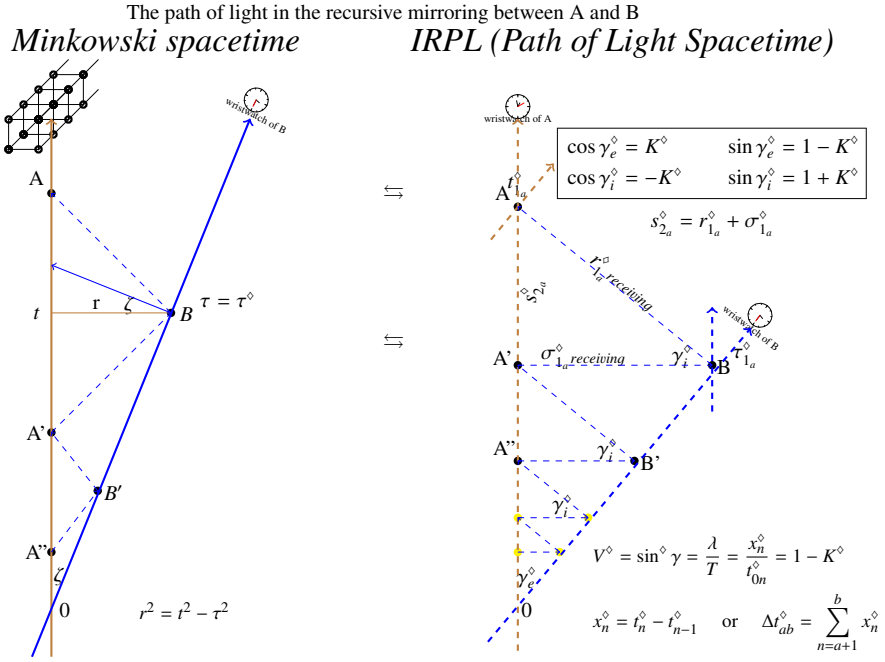

Fig. A3 isomorphism: in comparison the representations of the geometric progression $A, B, A', B', A'', B'', \ldots$ with $K^{\diamond}(\gamma)$ as the common ratio, deriving from the recursive mirroring of individuals A and B (see fig. A2). The IRPL diagram emerges from the historical reconstruction that connects the act of giving with the previous act of receiving and so on. Consequently, In the IRPL diagram the homologous frames, and therefore the homologous axes, face each other forming an angle γ (the heterologous frames, and therefore the heterologous axes give-riceive are in fact always parallel to each other).

Figure (A3) compares the representation of the progression of events $A, B, A', B', \ldots$ in Minkowski's spacetime with that in IRPL.

In a IRPL diagram, each segment arises from a geometric progression which has as its common ratio $\cos^{\diamond}\gamma$ and as scale factor a segment of a more primitive nature. Below the genesis of the spacetime (see fig.A4):

The core of a IRPL diagram consists of the radius of the two interacting individuals linked by the path of light during their interaction. In the interaction, the light path cyclically connects the head of each radius with the tail of the opposite radius, crossing the same radii.

starting from the above schema, indicating with:

$$R_a = \frac{G}{c^2} M_a \qquad R_{tot} = R_a + R_b \tag{A1a}$$

Since for each observer A, its proper mass at rest is opposed to the remaining masses B placed in their centre of gravity and subjected to the total gravitational field, the global energy-momentum Radius of A and B is

$$R^{\diamond}_{2_{Ab}} = 2\left(R_a + R_b \cos^{\diamond}\gamma\right) \qquad R^{\diamond}_{2_{Ba}} = 2\left(R_b + R_a \cos^{\diamond}\gamma\right) \tag{A1b}$$

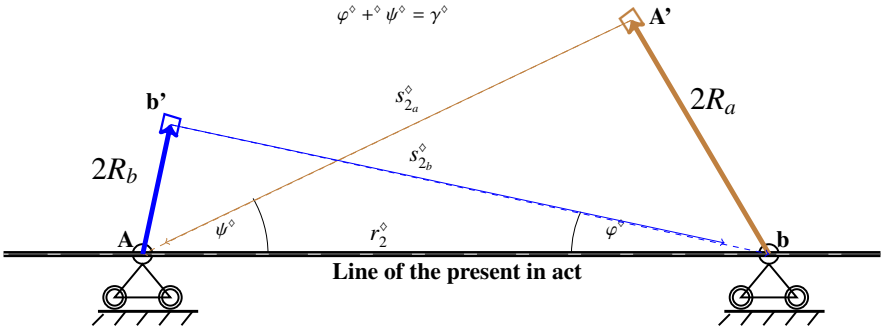

Fig. A4 the path of light: In the interaction, the light path cyclically connects the head of each radius with the tail of the opposite radius, crossing the same radii. The path between an emitter and a receiver is therefore equal to $r^\diamond_2 = 2r^\diamond = r^\diamond_a + r^\diamond_b = \vec{Ab} = 2R_a + s^\diamond_{2_a} = 2R_b + s^\diamond_{2_b} = 2(R_a + R_b)/\sin\gamma = 2R_a/\sin\psi = 2R_b/\sin\phi = 2(R_a + R_b)/(\sin\psi + \sin\phi)$.

and since a round trip route passes through both A and B, it descends that space and time proceed from mass-energy as follows:

$$R^\diamond_2 = \frac{R^\diamond_{2_{Ab}} + R^\diamond_{2_{Ba}}}{2} = R_{tot}(1 + \cos^\diamond\gamma) = R_{tot}\sin^\diamond\gamma_i \tag{A1c}$$

$$s^\diamond_2 = \sum_{-\infty}^{0} R^\diamond_{2_i} = R^\diamond_2\left(1 + \cos^\diamond\gamma + \cos^{\diamond 2}\gamma + \cdots\right) = \frac{R^\diamond_2}{\sin^\diamond\gamma_e} \tag{A1d}$$

$$r^\diamond = \sum_{-\infty}^{0} s^\diamond_{2_i} = s^\diamond_2\left(1 - \cos^\diamond\gamma + \cos^{\diamond 2}\gamma - \cdots\right) = \frac{s^\diamond_2}{\sin^\diamond\gamma_i} \tag{A1e}$$

$$\tau^\diamond = \sum_{-\infty}^{0} r^\diamond_i = r^\diamond\left(1 + \cos^\diamond\gamma + \cos^{\diamond 2}\gamma + \cdots\right) = \frac{r^\diamond}{\sin^\diamond\gamma_e} \tag{A1f}$$

where

$$s^\diamond_2 = \frac{s^\diamond_{2_a} + s^\diamond_{2_b}}{2} \qquad r^\diamond = \frac{r^\diamond_2}{2} = \frac{r^\diamond_a + r^\diamond_b}{2} \qquad \tau^\diamond = \frac{\tau^\diamond_a + \tau^\diamond_b}{2} \tag{A1g}$$

from the eq. (A1c, A1d, A1e, A1f) descends the fundamental relation:

$$V^\diamond = \quad R_{tot} : r^\diamond = r^\diamond : \tau^\diamond = \sin^\diamond\gamma_e \quad = p^\diamond/m \tag{A1h}$$

which expresses the "principle of equivalence, in the instant, between inertial and not inertial systems", see fig. (fig. A5).

Since the linear operators ($\sin^\diamond$, $\cos^\diamond$) are defined as the same ratios of the sides of a right triangle as the corresponding trigonometric functions, the rules for adding angles do not change. Indeed, denoting by $+^\diamond$ the reflective sum of two angles, we

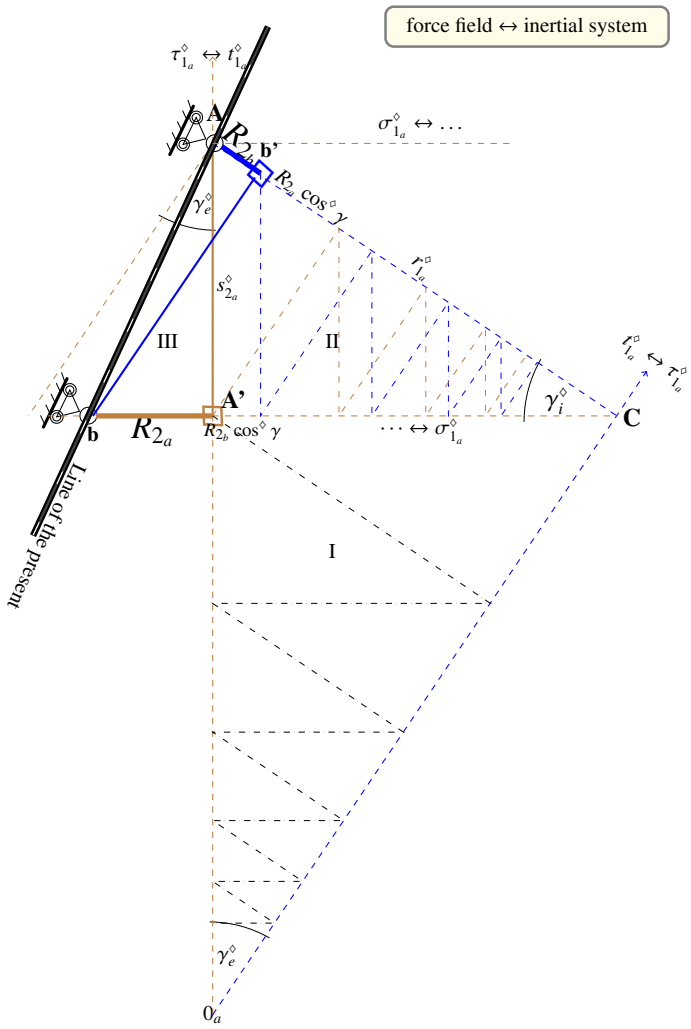

Fig. A5 The whole relation is enfolded and unfolds from the Radii of the two conjoined individuals with the dual angles γ_e and γ_i alternating each other. It is governed by the relation $R : r^{\diamond} = r^{\diamond} : \tau^{\diamond} = \sin^{\diamond}\gamma$. Indeed the three quadrants represent time, space and Radius and recursively follow one another. In particular the III-II quadrants represent the internal energy-space plane, while the II-I quadrants the external space-time plane.
The diagram represents the historical reconstruction of the relationship starting from the current instant. It coincides with real history only when γ is constant.

have $\gamma = (\varphi +^{\diamond} \psi) \neq (\varphi + \psi)$

$$\sin\left(\varphi \pm^{\diamond} \psi\right) = \sin^{\diamond}\varphi \pm \sin^{\diamond}\psi \qquad \cos\left(\varphi \pm^{\diamond} \psi\right) = \cos^{\diamond}\varphi \mp \sin^{\diamond}\psi \tag{A2a}$$

At last, it is easy to verify (see fig. A4) that:

$$r^{\diamond} = \frac{R_a + R_b}{\sin\gamma} = \frac{R_a}{\sin\psi} = \frac{R_b}{\sin\phi} = \frac{R_a + R_b}{\sin\psi + \sin\phi} = \frac{R_a + R_b}{\sin(\psi +^{\diamond} \phi)} \tag{A3}$$

A.2 The Electric universal

The universe would be composed solely of cold dark matter, uniformly distributed and subject to gravitation-electromagnetism, hitherto indistinguishable from each other, were it not for the fact that, for the very reason of being endowed with a finite Radius, it gives rise to a new special element, on which electromagnetism is much stronger than gravitation, and to radiation and therefore to all baryonic matter.

The following theses regarding the origin of baryonic matter and its distinctive properties flow naturally from the standpoint of light geometry as follows:

Thesis 3 *Coexistence and relationship between electromagnetism and gravitation: given that, in the relationship, each of the two individuals has, in addition to its own "proper" gravitational Radius* $R_{\bullet}$*, the "reflected in the other" electric Radius* R° *of its other, the electric Radius* R° *is the inverse of the gravitational Radius* $R_{\bullet}$ *of the other*

$$R^{\circ}_{a} = R^{-1}_{\bullet b} \tag{A4}$$

Indeed, since the hypothesis (1) demands that the global angle γ splits in two angles $\gamma = \phi +^{\diamond} \psi$ (see fig. A4) such that:

$$\lambda_a = 2\pi\frac{R^{\circ}{}_{b}}{\sin^{\diamond}\varphi} = 2\pi\frac{R^{\circ}{}_{b}}{V^{\diamond}_{a}} \qquad = \lambda_b = 2\pi\frac{R^{\circ}{}_{a}}{\sin^{\diamond}\psi} = 2\pi\frac{R^{\circ}{}_{a}}{V^{\diamond}_{b}} \qquad = 2\pi r^{\diamond} \tag{A5}$$

and, in addition, from the De Broglie relation $\lambda = h/p$ we have:

$$\lambda_a = 2\pi\hbar\frac{1/m_a}{p_a/m_a} \qquad = \lambda_b = 2\pi\hbar\frac{1/m_b}{p_b/m_b} \qquad = 2\pi r^{\diamond} \tag{A6}$$

since $V^{\diamond} = p^{\diamond}/mc$, it follows the thesis (3).

The first relationship is the "part of" relation between the universe and the element of cold dark matter that we call Amorone.

Although it is a continuous and uniform whole, the universe is cyclical. Since light cross the Radius in every interaction, it has a "proper" Radius $R_{\bullet} = c/H_0 = R_{\Omega}$ and a "reflected in the other" Radius $R^{\circ} = R^{-1}_{\Omega} = H_0/c = R_{\alpha}$ which correspond to Universe's and Amorone's Radius, gravitational and electrical Radius, gravitational and electric period, potency and act, Radius and space. Therefore it is almost always in potency as Universe, almost always in act as Amorone. Its three axes constituted by the Radius of the universe, i.e. the power and the maximum, the Radius of the Amorone, i.e. the act and the minimum, and the space that connects them, i.e. the radiation, are reduced almost exclusively to the Radius of universe or of the radiation almost overlapping in the opposite direction. For both universe and its element, we have $R_{\bullet} = R^{\circ}$, that is coincidence between gravitation and electromagnetism.

At last

Thesis 4 *The birth of the Electric Universal: There is, and is unique, a special individual within the universe such that its gravitational Radius $R_\bullet$ is exactly equal to the mass contained in its electric Radius R°:*

$$R_\bullet : R^\circ = R^\circ : R_{\Omega_b} \tag{A7}$$

where $R^\circ = R_\bullet^{-1}$ and $R_{\Omega_b} = R_\Omega/\Omega_b$ and where $l_{irpl} = 2\sqrt{\alpha}\, l_p$ and $m_{irpl} = \sqrt{\alpha}\, m_p$ (l_p and m_p are the Planck length and mass). This special individual which, in the various forms it takes on the basis of position and combination, gives rise to all baryonic matter, is the electron:

$$\left(\frac{2m_e}{m_{irpl}}\right)^{-3} l_{irpl} = \frac{R_\Omega}{\Omega_b} \tag{A8}$$

. That is, the composite (gravitationally) elementary (electrically) individual R_ϵ, with its three generations, is the building block of all matter, leptons, quarks and bosons, since it is sole individual that is in equilibrium with universe

Follows immediately from thesis (4) the universality of electric spin

Thesis 5

$$Spin = R_\bullet c R^\circ/2 = 1/2 \tag{A9}$$

which is the parallel of the extreme gravitational angular momentum $j = R_\bullet^2$ of a black hole.

Along the path, the fine structure constant is the equivalent of Euclidean π. That is

Thesis 6 *Every individual advances over time by rotating in the plan of potency as a screw with pitch α^{-1}.*

The electron plays, in the field of electrical interactions, a role similar to that of the Universe in the field of gravitational interactions. It has gravitational period $R_{\bullet e}$ and electrical period R_e°.

Thesis 7 *the mass/energy present within the electric Radius ($r^\diamond = \sin^\diamond \gamma\, R_e^\circ \leq R_e^\circ$) is that of cold dark matter $R_\bullet = r^{\diamond 2}/R_{\Omega_b} = \sin^{\diamond 2}\gamma\, R_{\bullet e}$. This constraints the mass of neutrinos and of quarks*

Thesis 8 *In a dual way to what happens for gravitation and inertia, the agreement with the experience requires that for electric fields:*

$$\cos^\diamond \gamma = \cos\gamma \tag{A10}$$

that is the energy, i.e. Balmer's radiation, bosons $W^\pm$, Z_0, mesons, X, γ radiation, depends on the cosine

$$\Delta E_{n1}^{n2} = m_e \left(\Delta \cos\left(j\pi \pm \frac{\alpha}{n}\right)\right)^{\pm 1} \tag{A11}$$

where m_e is the mass of the electron, $j = 0, 1/2, 1$ respectively in the Coulomb, strong and weak interactions and where the exponent is positive outside the Radius (Coulomb interactions), negative otherwise.

With the birth of the electric universal and of the consequent baryonic matter, the three axes of the Universe are no longer almost overlapping. Now, each of the three axes of the universe: Power, Act, Radiation, corresponds respectively to an energy component: $\Omega = \Omega_c + \Omega_b + \Omega r$. The definition of the relationship (1) suggests:

Thesis 9 *The three different generations of the matter come from the axis of the universe on which the temporal axis of the individual is aligned:*

$$\Omega_c : \Omega_b : \Omega_r \sim m_e^{-1} : m_\mu^{-1} : m_\tau^{-1} \sim \|V_{\mathrm{ud}}\|^2 : \|V_{\mathrm{cd}}\|^2 : \|V_{\mathrm{td}}\|^2 \sim \dots \tag{A12}$$

Thesis 10 *The three axes correspond to the three fundamental symmetry operations in particle physics:*

$S_\parallel$	$r^\diamond$	*Momentum*	***P**arity*	*reverses signs of space coordinates*
$\boldsymbol{T}$	$t^\diamond$	*Energy*	***T**ime reversal*	*reverses sign of time coordinate*
$S_\perp$	R	*Radius*	***C**harge conjugation*	*exchanges particle and antiparticle*

$$CP \equiv T \qquad CT \equiv P \qquad PT \equiv C \qquad CPT \equiv 1$$

Furthermore, it is easy to verify that in the linear geometry of the act it turns out

Thesis 11 *The sum of two angles $\pi/3$ gives rise to a right angle: $\pi/3 +^\diamond \pi/3 = \pi/2$. Indeed:*

$$\sin^\diamond \pi/3 + \sin^\diamond \pi/3 = 2(1 - \cos \pi/3) = 1 = \sin^\diamond(\pi/3 +^\diamond \pi/3) = \sin^\diamond \pi/2 \tag{A13}$$

This property establishes the constitution of baryons from a ternary relation in the strong interaction area where the angle γ between each pair is $\pi/2$. In other words, while the weak interaction is the relationship between an individual and its anti on opposite sides of the same axis, the strong interaction is the triadic relationship that takes place at the crossing point of the three axes of space, potency, act and radiation, between of them perpendicular, in which the three pairs arranged at $(\pi/3 +^\diamond \pi/3) + (\pi/3 +^\diamond \pi/3) + (\pi/3 +^\diamond \pi/3)$ relate.

Since gravitation takes place in the power between cdm, the matter-antimatter distinction and the consequent give-receive, is relevant only during the electric cycle of an electric individual.

The distinction between matter and antimatter is relative as each individual moves from one form to another continually during its spin cycle. Similarly, the polarising distinction between sender and receiver is just apparent and deceptive because both individuals send and receive simultaneously in the same act. Said A^- the matter and A^+ the antimatter, both A^- and A^+ send a part of themselves in the same act, the matter going forward in time from the sender A^- to the receiver A^+, the antimatter going backward in time from the receiver A^- to the sender A^+, so that they form a neutral boson where the component parts proceed hand in hand from the sender as matter to the receiver as antimatter. Between two homologous individuals, vice versa,

the two parties sent proceed in the opposite direction, which has the opposite effect of attraction.

Thesis 12 *Universal electric Rotation period: all electric individuals share the same Rotation period, in such a way as to generate a relative partition between the set of matter individuals and the dual set of anti-matter individuals. In order to reverse the relative matter-antimatter direction with respect to the other individuals, the individual would have to reverse its axes, ie exceed the speed of light with respect to the other individuals. This universal property of the electron, in all its generations, is the electric charge, which is conventionally negative for matter and positive for antimatter. As a result, each electric individual counts for one (charge* ± 1*). The exception is quarks, which exist as such only in the strong interaction, where each individual component, each arranged on one of the three axes of space converging at the point* $\gamma = \pi/2$*, counts for* $\pm 1/3$*, because it is free to interact only one time out of three, in accordance with the cyclical alternation of its three moments (PotencyEnergyAct). Each moment corresponds to a colour of chromodynamics.*

The charge of an aggregate is the relative sum of the component individuals. Consequently, the equivalence between positive and negative charges is equivalent to a corresponding equivalence between matter and antimatter. In the case of an electric interaction, the electric Radius is given by adding the reflection of the other's gravitational Radius in each of its constituent component individuals, the relative number of which is known as the resultant electric charge.

From these assumptions it follows that neutrinos, as they are electrically neutral, are constituted by a couple matter-antimatter $(-1, +1)$ linked via weak interaction. Analogously, the quarks Up are supposed to be constituted by a couple of individuals matter-antimatter $(-1/3, +1)$ where only one is engaged in the strong interaction, the one with charge $-1/3$, while the other is linked to this via weak interaction, far away, and therefore does not interfere with the strong interaction and has charge $+1$.

As a result, Coulomb interactions, which take place outside the Radius, typically occur between an electron of mass $m = m_e \simeq 0.511 MeV$ and its reflection in the nucleus which assumes electric Radius $R = R_e^\circ \simeq 2.81794 fm$ (the vice-versa is negligible). On the other hand, weak and strong interactions, which take place inside the Radius between leptons, typically occur between an electron of augmented mass $m = \pi m_e \simeq 1.60535 MeV$ and its reflection in the other lepton conjoined in the relationship, which assumes electric Radius $R = R_e^\circ/\pi \simeq 0.896978 fm$ (see fig.A7). All electrical interactions share $L/c = n/\alpha$.

At last, all systems, whether gravitational or electric (or inertial), share the universal metric illustrated in the next section.

A.3 The universal metric

While the spin is the rotation around the time axis (in the plane of potency), the circular motion is due to an inclination by a nutation angle ϑ of the Euclidean time-power plane around the axis of the nodes $r^\diamond$. Consequently, the γ angle decomposes according to its component frames $\gamma = \varphi +^\diamond \psi$.

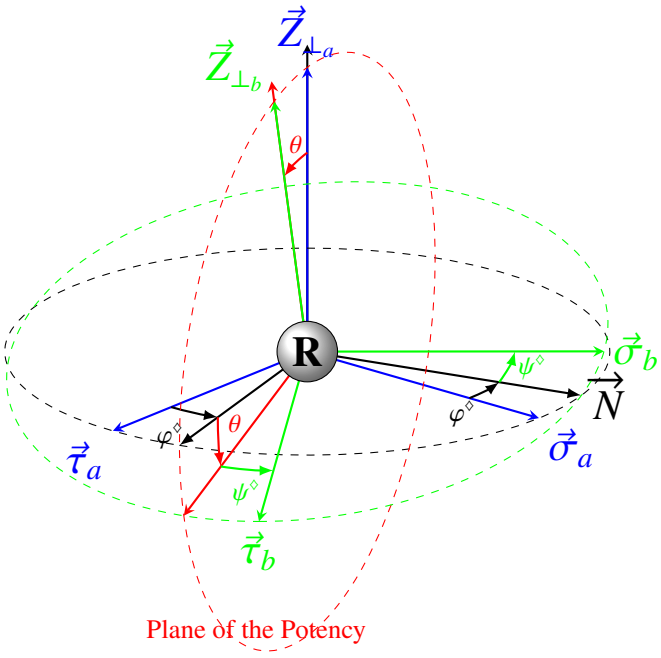

Fig. A6 The two reference frames weave around the axis of the nodes $r^\diamond$ decomposing the γ angle according to its component frames $\gamma = \varphi +^\diamond \psi$.

$$\begin{bmatrix} d\sigma^\diamond \\ id\tau^\diamond \\ \sigma^\diamond d\phi \end{bmatrix} = \begin{bmatrix} \cos^\diamond\varphi & \sin^\diamond\varphi & 0 \\ -\sin^\diamond\varphi & +\cos^\diamond\varphi & 0 \\ 0 & 0 & 1 \end{bmatrix} \begin{bmatrix} 1 & 0 & 0 \\ 0 & \cos\vartheta & +\sin\vartheta \\ 0 & -\sin\vartheta & \cos\vartheta \end{bmatrix} \begin{bmatrix} \cos^\diamond\psi & \sin^\diamond\psi & 0 \\ -\sin^\diamond\psi & +\cos^\diamond\psi & 0 \\ 0 & 0 & 1 \end{bmatrix} \begin{bmatrix} dx^\diamond \\ idt^\diamond \\ r^\diamond d\phi \end{bmatrix} \tag{A14}$$

$$\begin{bmatrix} d\sigma^\diamond \\ id\tau^\diamond \\ \sigma^\diamond d\phi \end{bmatrix} = Z_1 X_2 Z_3 = \begin{bmatrix} c_1c_3 - c_2s_1s_3 & -c_1s_3 - c_2c_3s_1 & s_1s_2 \\ c_3s_1 + c_1c_2s_3 & c_1c_2c_3 - s_1s_3 & -c_1s_2 \\ s_2s_3 & c_3s_2 & c_2 \end{bmatrix} \begin{bmatrix} dx^\diamond \\ idt^\diamond \\ r^\diamond d\phi \end{bmatrix} \tag{A15}$$

where s and c represent sine and cosine (e.g., s_1 represents the sine of φ) and

$$\cos\xi = \cos(\varphi + \psi) = \frac{1}{1 - V^\diamond} \tag{A16}$$

$$\tan\vartheta = i\frac{(L+J)/m}{r} = i\frac{a}{r} = \sqrt{\frac{1}{\cos^2\vartheta} - 1} \tag{A17}$$

Since

$$dx^\diamond = -v^\diamond i\, dt^\diamond + dr^\diamond = -\left(\frac{a_{12}}{a_{11}} idt^\diamond + \frac{a_{13}}{a_{11}} r^\diamond d\phi\right) + dr^\diamond \tag{A18}$$

we have:

$$\left[d\vec{l}^{\diamond}\right] = \begin{bmatrix} d\sigma^{\diamond} \\ id\tau^{\diamond} \\ \sigma^{\diamond} d\phi \end{bmatrix} = \left(\begin{bmatrix} a_{11} & 0 & 0 \\ a_{21} & a_{22} & a_{23} \\ a_{31} & a_{32} & a_{33} \end{bmatrix} - \begin{bmatrix} 0 & 0 & 0 \\ 0 & a_{21}\frac{a_{12}}{a_{11}} & a_{21}\frac{a_{13}}{a_{11}} \\ 0 & a_{31}\frac{a_{12}}{a_{11}} & a_{31}\frac{a_{13}}{a_{11}} \end{bmatrix} \right) \begin{bmatrix} dr^{\diamond} \\ idt^{\diamond} \\ r^{\diamond} d\phi \end{bmatrix} \tag{A19}$$

At last, since

$$dR = V^{\diamond}\, dr^{\diamond} = -(a_{21} + a_{31}) dr^{\diamond} \tag{A20}$$

and along the path of light $d\vec{l}^{\diamond} = 0$, it results:

$$\left[d\vec{R}^{\diamond}\right] = -\begin{bmatrix} 0 \\ a_{21} \\ a_{31} \end{bmatrix} dr^{\diamond} = \begin{bmatrix} p_{rr} & 0 & 0 \\ 0 & \mathbb{E}_{tt} & p_{t\vartheta} \\ 0 & \mathbb{E}_{\vartheta t} & p_{\vartheta\vartheta} \end{bmatrix} \begin{bmatrix} dr^{\diamond} \\ idt^{\diamond} \\ r^{\diamond} d\phi \end{bmatrix} \tag{A21}$$

This general metric can be expressed in the general form:

$$\pm i\vec{\mathrm{k}}\mathbb{E} \pm \vec{\mathrm{i}}p + \vec{\mathrm{j}}m = 0 \tag{A22}$$

or specialized for electric and gravitational interactions:

$$\left(\gamma^{\mu}\partial_{\mu} + im\right)\psi = 0 \qquad\qquad R_{\mu\nu} - \frac{1}{2} g_{\mu\nu} R = \frac{8\pi G}{c^4} T_{\mu\nu} \tag{A23}$$

In particular, when the angle $\psi^{\diamond} = 0$ ($c_3 = 1,\ s_3 = 0$) we have the Kerr Metric:

$$\left[d\vec{R}^{\diamond}\right] = -\begin{bmatrix} 0 \\ s_1 \\ 0 \end{bmatrix} dr^{\diamond} = \left(\begin{bmatrix} c_1 & 0 & 0 \\ 0 & c_1 c_2 & -c_1 s_2 \\ 0 & s_2 & c_2 \end{bmatrix} - \begin{bmatrix} 0 & 0 & 0 \\ 0 & s_1 \frac{-c_2 s_1}{c_1} & s_1 \frac{s_1 s_2}{c_1} \\ 0 & 0 & 0 \end{bmatrix} \right) \begin{bmatrix} dr^{\diamond} \\ idt^{\diamond} \\ r^{\diamond} d\phi \end{bmatrix} \tag{A24}$$

$$\frac{-d\vec{R}}{\cos\vartheta} \equiv \frac{1}{\cos\vartheta} \frac{dr}{(V_i - 1)} \hat{\mathbf{e}}_r + \{idt\,(1 - V_e) - rd\phi\,(1 - V_e)\tan\vartheta\}\,\hat{\mathbf{e}}_t + \{idt\tan\vartheta + rd\phi\}\,\hat{\mathbf{e}}_{\phi} \tag{A25}$$

and squaring (from the (A17) $\tan\vartheta = ia/r$ and $1/\cos\vartheta = \sqrt{1 - a^2/r^2}$):

$$\begin{aligned} dR^2 = (1 - 2V)\, dt^2 + 4\frac{a}{r} V r d\phi dt - \frac{dr^2}{(1 - V^{\diamond})^2} - \left(1 + \frac{a^2}{r^2} + 2V\frac{a^2}{r^2}\right) r^2 d\phi^2 + \\ + \frac{a^2}{r^2}\left[dR^2 + \frac{dr^2}{1 - 2V} - c^2 dt^2\right] \end{aligned} \tag{A26}$$

where the term in square brackets is $\left[\left(\sin^2\varphi + \cos^2\varphi\right) dr^{\diamond 2} - c^2 dt^{\diamond 2}\right] = dr^{\diamond 2} - c^2 dt^{\diamond 2}$.

On the other hand, when $\phi = 0\,(c_1 = 1,\ s_1 = 0)$ we have the Schwarzchild Metric:

$$\left[d\vec{R}^{\diamond}\right] = -\begin{bmatrix} 0 \\ c_2 s_3 \\ s_2 s_3 \end{bmatrix} dr^{\diamond} = \left(\begin{bmatrix} c_3 & 0 & 0 \\ 0 & c_2 c_3 & -c_1 s_2 \\ 0 & c_3 s_2 & c_2 \end{bmatrix} - \begin{bmatrix} 0 & 0 & 0 \\ 0 & c_2 s_3 \frac{-s_3}{c_3} & 0 \\ 0 & s_2 s_3 \frac{-s_3}{c_3} & 0 \end{bmatrix}\right) \begin{bmatrix} dr^{\diamond} \\ idt^{\diamond} \\ r^{\diamond} d\phi \end{bmatrix} \tag{A27}$$

$$-dR\left(\cos\vartheta\,\hat{\mathbf{e}}_t + \sin\vartheta\,\hat{\mathbf{e}}_\phi\right) \equiv \frac{dr^{\diamond}}{1 - V^{\diamond}}\hat{\mathbf{e}}_r + \left\{idt^{\diamond}(1 - V^{\diamond})\cos\vartheta - r^{\diamond} d\phi \sin\vartheta\right\}\hat{\mathbf{e}}_t + \\ + \left\{idt^{\diamond}(1 - V^{\diamond})\sin\vartheta + r^{\diamond} d\phi \cos\vartheta\right\}\hat{\mathbf{e}}_\phi \tag{A28}$$

and squaring:

$$dR^2 = c^2 dt^{\diamond 2}(1 - V^{\diamond})^2 - \frac{dr^{\diamond 2}}{(1 - V^{\diamond})^2} - r^{\diamond 2} d\phi^2 \tag{A29}$$

where, substituting the two constants of motion $r^{\diamond 2} d\phi/d\tau = L/m$ and $dt^{\diamond} = E/(mc^2)\, d\tau/(1 - V^{\diamond})^2$

$$\mathbf{U} = \frac{1}{2} mc^2 \left[-2V^{\diamond} + V^{\diamond 2} + \left(\frac{dr^{\diamond}}{d\tau}\right)^2 + \frac{L^2 V_{\vartheta}^{\diamond 2}}{m^2 R^2 c^2}\left(1 - V^{\diamond}\right)^2\right] \tag{A30}$$

where

- for gravitational interactions, the $V^{\diamond}$ is usually replaced by the V via the (24) giving the Schwarzschild metric;
- the potential $V^{\diamond} = \sin\gamma^{\diamond} \leq 1$, reverses from outside $V^{\diamond} = R/r^{\diamond}$ to inside $V^{\diamond} = r^{\diamond}/R$;
- for electric and for the inside of gravitational interactions, it holds $mR = R_{\bullet} R^{\circ} = 1$;
- all electrical interactions share $L/c = n/\alpha$
- the pseudo potential $V_{\vartheta}^{\diamond}$ term is equal to $V_{\vartheta}^{\diamond} = R/r^{\diamond}$ when the native seat of the relationship is outside R, to $V_{\vartheta}^{\diamond} = r^{\diamond}/R$ otherwise. But, contrarily to the potential $V^{\diamond}$, its formula does not reverse but continues to grow when the distance $r^{\diamond}$, overflowing its seat, crosses the threshold R.
  It is the conservation of angular momentum, therefore, that determines the confinement of the relationship on one side or the other of Radius R in the strong interaction.

A.4 The meaning of IRPL and its relationship with Minkowski's spacetime

The physical representation in Minkowski/Riemannian manifold spacetime and that in the IRPL, although completely different, as deriving from two completely different metaphysics, are isomorphic to each other. Which of the two is the real one (or the more primitive) is not a matter of taste, rather of criteria of naturalness, simplicity and generality.

According to the physicist John Wheeler, Einstein's general theory of relativity can be summed up in just 12 words: *"Space-time tells matter how to move; matter tells space-time how to curve"*.

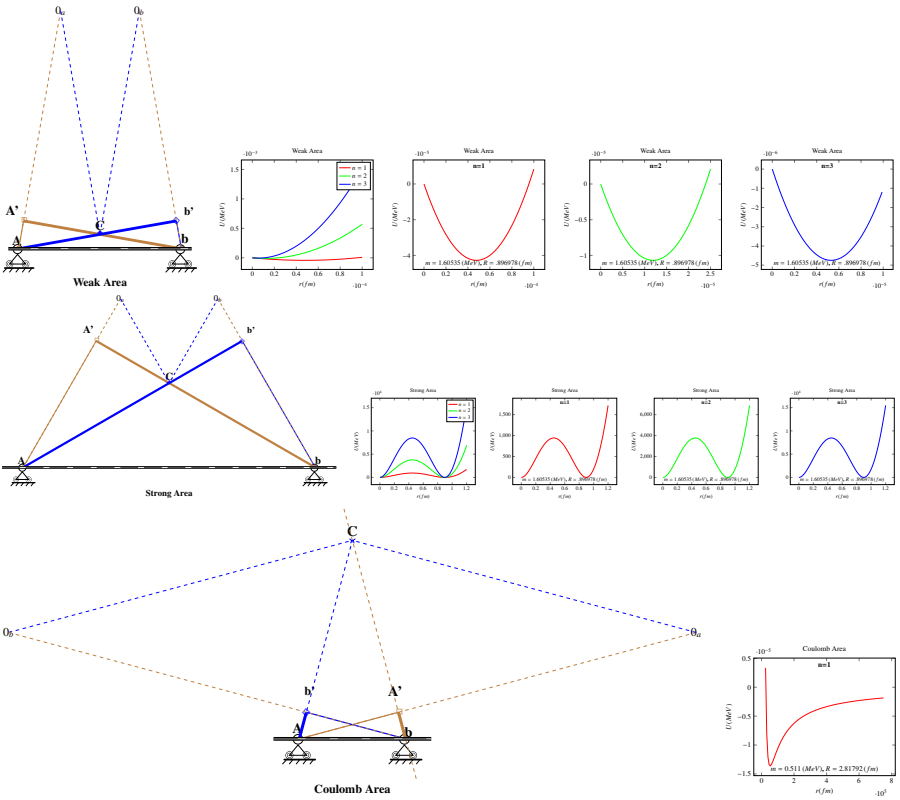

Fig. A7 From top to bottom the electrical potential (A30) respectively for weak, strong and Coulomb interactions.

IRPL removes absolute spacetime: "matter tells matter how to move in the potency". More precisely, IRPL also removes matter. In fact, the universe is the set of the totality of individuals in relation to each other where each individual (the elementary individual is the quantum of matter) is distinguished by its position with respect to the others.

The IRPL diagram is only a knowledge representation system, it emerges reflexively (probabilistically) from the potency by means of the same theory on which QED is based, when the uncertainty inherent in IRPL (see. fig. A1) dissolves. It is therefore the reality that lies beneath the Riemannian manifold that reflexively (phenomenologically) emerges from it, and the ground that unifies gravitation with quantum mechanics and inertial systems.

Gravity is the potential relation. It is the background, the foundation. As in potentiality, it does not occur between a given this in act and a given other in act, and it does not exchange real bosons in act for the same reason. It does not appear, it is not a phenomenon, it is the fundamental internal and underlying relationship to the universe. On the foundation of gravity, in the space that it constitutes within the universe, the electrical relation emerges. It is, on the contrary, in act and constitutes the phenomenon. It takes place between a determined one and another determined one by

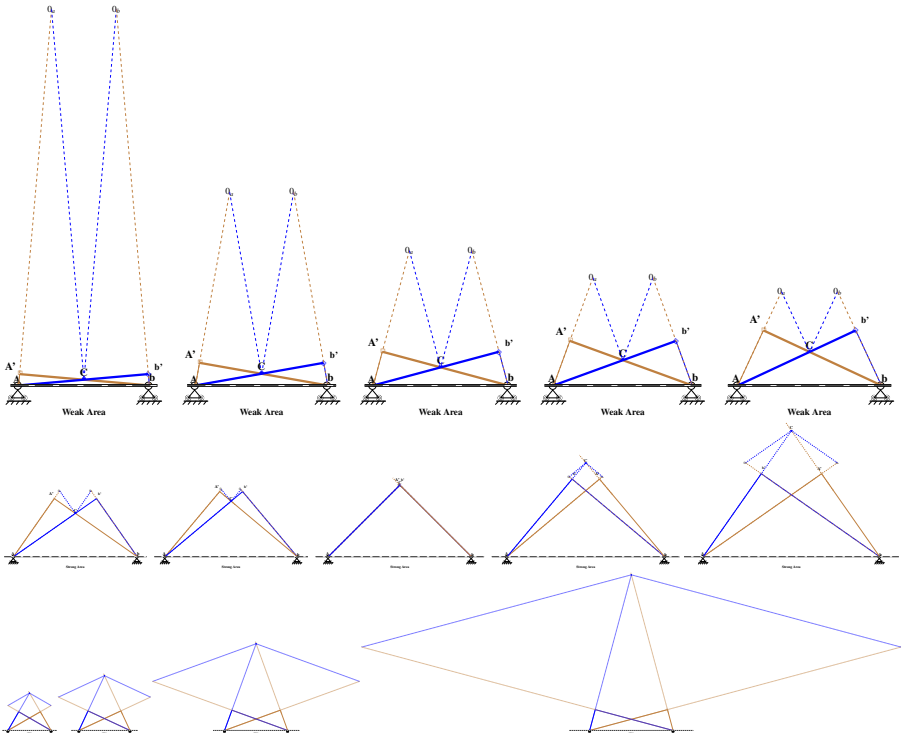

Fig. A8 The evolution of the universal diagram of the relationship from interactions within the Radius, above, through the surface, in the center, and finally outside it, below.

means of an exchange of bosons in act. It is the Coulomb or, alternately, the Strong or Weak interaction, depending on whether the relationship occurs externally to the Radii of the involved individuals or internally to the Radius of the whole. Indeed, gravity and electricity are to each other as the soul and consciousness. The universe thinks and behaves by generating the physical world which is not the Euclidean one. Euclidean geometry is abstract and intellectual, it is a meta-thought, it is human thought which is generated and which meditates on the thought of nature.

Table A1 IRPL parameters that satisfy the constraints 1,2,3
the table shows, as the baryon density varies, the values assumed by the parameters of the IRPL model that satisfy the first five constraints. It should be noted that the redshift z^* that satisfies the constraint of the acoustic angular scale coincides with that calculated by CAMB based on the baryon and CDM densities at z^*

	IRPL values satisfying constraints 1,2,3					CAMB input		CAMB output	CAMB input		CAMB output
ω_{0_b}	H_0	z^*	r^*	z_d	r_{drag}	$\omega_{bs}(z^*)$	$\omega_{cs}(z^*)$	z^*	$\omega_{bs}(z_d)$	$\omega_{cs}(z_d)$	z_d
...	...	...	...	...	...	...	...	...	...	...	...
0.022	73.63	1138.15		1034.0		0.010332	0.244284	1138.03	0.010302	0.243574	1034.03
0.02205	73.63	1138.00		1034.1		0.010355	0.244216	1137.88	0.010325	0.243508	1034.12
0.0221	73.62	1137.84		1034.2		0.010379	0.244148	1137.73	0.010348	0.243441	1034.22
0.02215	73.61	1137.69		1034.3		0.010402	0.244080	1137.58	0.010372	0.243375	1034.32
0.0222	73.61	1137.53		1034.4		0.010425	0.244012	1137.43	0.010395	0.243309	1034.42
0.02225	73.60	1137.38		1034.5		0.010449	0.243945	1137.28	0.010419	0.243243	1034.51
0.0223	73.60	1137.22		1034.6		0.010472	0.243877	1137.13	0.010442	0.243178	1034.61
0.02235	73.59	1137.07		1034.7		0.010496	0.243809	1136.98	0.010466	0.243112	1034.71
0.0224	73.58	1136.91		1034.8		0.010519	0.243742	1136.83	0.010489	0.243047	1034.80
0.02245	73.58	1136.76		1034.9		0.010543	0.243675	1136.68	0.010513	0.242981	1034.90
0.0225	73.56	1136.51	129.3	1035.2	137.67	0.010566	0.243534	1136.51	0.010536	0.242844	1035.27
0.02255	73.56	1136.45		1035.0		0.010589	0.243541	1136.39	0.010559	0.242850	1035.09
0.0226	73.56	1136.29		1035.1		0.010613	0.243474	1136.24	0.010583	0.242785	1035.19
0.02265	73.55	1136.14		1035.2		0.010636	0.243407	1136.09	0.010606	0.242720	1035.28
0.0227	73.55	1135.98		1035.3		0.010660	0.243340	1135.94	0.010630	0.242655	1035.38
0.02275	73.54	1135.83		1035.4		0.010683	0.243273	1135.79	0.010653	0.242590	1035.48
0.0228	73.53	1135.68		1035.57		0.010707	0.243207	1135.64	0.010677	0.242526	1035.58
0.02285	73.53	1135.53		1035.67		0.010731	0.243141	1135.49	0.010701	0.242462	1035.67
0.0229	73.52	1135.37		1035.76		0.010754	0.243074	1135.35	0.010724	0.242397	1035.77
0.02295	73.52	1135.22		1035.86		0.010778	0.243008	1135.2	0.010748	0.242333	1035.86
0.023	73.51	1135.07		1035.95		0.010801	0.242942	1135.05	0.010771	0.242268	1035.95
0.02305	73.5	1134.91		1036.05		0.010824	0.242876	1134.9	0.010794	0.242204	1036.05
0.0231	73.5	1134.76		1036.14		0.010848	0.242810	1134.75	0.010818	0.242140	1036.14
0.02315	73.49	1134.61		1036.24		0.010871	0.242744	1134.6	0.010841	0.242076	1036.24
0.0232	73.49	1134.45		1036.33		0.010895	0.242678	1134.45	0.010865	0.242012	1036.33
0.02325	73.48	1134.3	129.44	1036.43	137.52	0.010918	0.242612	1134.3	0.010888	0.241948	1036.42
0.0233	73.47	1134.15		1036.52		0.010942	0.242547	1134.15	0.010912	0.241884	1036.52
0.02335	73.47	1133.99		1036.61		0.010965	0.242481	1134	0.010935	0.241820	1036.61
0.0234	73.46	1133.84		1036.71		0.010988	0.242416	1133.85	0.010959	0.241757	1036.71
0.02345	73.46	1133.69		1036.8		0.011012	0.242350	1133.7	0.010982	0.241693	1036.8
0.0235	73.45	1133.54		1036.89		0.011035	0.242285	1133.55	0.011005	0.241630	1036.89
0.02355	73.44	1133.38		1036.99		0.011059	0.242220	1133.4	0.011029	0.241566	1036.99
0.0236	73.44	1133.23		1037.08		0.011082	0.242155	1133.25	0.011052	0.241503	1037.08
0.02365	73.43	1133.08		1037.17		0.011106	0.242090	1133.11	0.011076	0.241440	1037.17
0.0237	73.43	1132.93		1037.26		0.011129	0.242025	1132.96	0.011099	0.241377	1037.26
0.02375	73.42	1132.78		1037.36		0.011152	0.241960	1132.81	0.011123	0.241314	1037.36
0.0238	73.42	1132.63		1037.45		0.011176	0.241896	1132.66	0.011146	0.241251	1037.45
0.02385	73.41	1132.47		1037.54		0.011199	0.241831	1132.51	0.011170	0.241188	1037.54
0.0239	73.4	1132.32		1037.63		0.011223	0.241767	1132.36	0.011193	0.241126	1037.63
0.02395	73.4	1132.17		1037.72		0.011246	0.241702	1132.21	0.011216	0.241063	1037.72
0.024	73.39	1132.02		1037.82		0.011270	0.241638	1132.06	0.011240	0.241000	1037.81
0.02405	73.39	1131.87		1037.91		0.011293	0.241574	1131.91	0.011263	0.240938	1037.91
0.0241	73.38	1131.72		1038		0.011317	0.241510	1131.76	0.011287	0.240876	1038
0.02415	73.37	1131.57		1038.09		0.011340	0.241446	1131.61	0.011310	0.240813	1038.09
0.0242	73.37	1131.42		1038.18		0.011363	0.241382	1131.46	0.011334	0.240751	1038.18
...	...	...	...	...	...	...	...	...	...	...	...

Table A2 [37] find that every model which satisfies $100\omega_b = 2.13 \pm 0.05$, $\omega_c = 0.124 \pm 0.007$, $n_s = 0.93 \pm 0.02$, $\theta^* = 0.593° \pm 0.001°$ will automatically be in agreement with the CMB data for $\ell \geq 40$. Only lower ℓ CMB data, large scale structure, lensing and other observations can distinguish between models which have the above values for ω_b, ω_c, n_s and θ^*

			CAMB input parameters for TT, TE and EE power spectra					
ω_{0_b}	η	z^*	H_0	$\omega_b(\theta^* = 0.0104109)$	$\omega_b(z^*)$	$\omega_c(z^*)$	$\omega_m(z^*)$	He/H
...	...	...	...	...	...	...	...	...
0.02195	6.00925×10^{-10}	1138.3	73.63	0.02106	0.00516	0.12221	0.12737	
0.022	6.02294×10^{-10}	1138.1	73.63	0.02111	0.00517	0.122175	0.12734	
0.02205	6.03663×10^{-10}	1138.0	73.62	0.02116	0.00518	0.122141	0.12732	
0.0221	6.05032×10^{-10}	1137.8	73.62	0.02121	0.00519	0.122107	0.1273	
0.02215	6.06401×10^{-10}	1137.6	73.61	0.02126	0.00520	0.122073	0.12728	
0.0222	6.07769×10^{-10}	1137.5	73.6	0.0213	0.00522	0.122039	0.12725	
0.02225	6.09138×10^{-10}	1137.3	73.6	0.02135	0.00523	0.122006	0.12723	0,2442
0.0223	6.10507×10^{-10}	1137.2	73.59	0.0214	0.00524	0.121972	0.12721	
0.02235	6.11876×10^{-10}	1137.0	73.58	0.02145	0.00525	0.121938	0.12719	
0.0224	6.13245×10^{-10}	1136.9	73.58	0.0215	0.00526	0.121904	0.12717	
0.02245	6.14614×10^{-10}	1136.6	73.56	0.02154	0.00527	0.121833	0.12711	
0.0225	6.15983×10^{-10}	1136.6	73.57	0.02159	0.00529	0.121837	0.12712	
0.02255	6.17351×10^{-10}	1136.4	73.56	0.02164	0.00530	0.121803	0.1271	
0.0226	6.18720×10^{-10}	1136.2	73.55	0.02169	0.00531	0.12177	0.12708	0,2444
0.02265	6.20089×10^{-10}	1136.1	73.55	0.02174	0.00532	0.121736	0.12706	
0.0227	6.21458×10^{-10}	1135.9	73.54	0.02178	0.00533	0.121703	0.12704	
0.02275	6.22827×10^{-10}	1135.8	73.53	0.02183	0.00534	0.12167	0.12701	
0.0228	6.24196×10^{-10}	1135.6	73.53	0.02188	0.00536	0.121636	0.12699	
0.02285	6.25564×10^{-10}	1135.5	73.52	0.02193	0.00537	0.121603	0.12697	
0.0229	6.26933×10^{-10}	1135.3	73.52	0.02198	0.00538	0.12157	0.12695	
0.02295	6.28302×10^{-10}	1135.2	73.51	0.02202	0.00539	0.121537	0.12693	
0.023	6.29671×10^{-10}	1135.0	73.5	0.02207	0.00540	0.121504	0.12691	0,2446
0.02305	6.31040×10^{-10}	1134.9	73.5	0.02212	0.00541	0.121471	0.12689	
0.0231	6.32409×10^{-10}	1134.7	73.49	0.02217	0.00543	0.121438	0.12686	
0.02315	6.33778×10^{-10}	1134.6	73.49	0.02222	0.00544	0.121405	0.12684	
0.0232	6.35146×10^{-10}	1134.4	73.48	0.02226	0.00545	0.121372	0.12682	
0.02325	6.36515×10^{-10}	1134.3	73.48	0.02231	0.00546	0.121342	0.1268	
0.0233	6.37884×10^{-10}	1134.1	73.47	0.02236	0.00547	0.121306	0.12678	
0.02335	6.39253×10^{-10}	1133.9	73.46	0.02241	0.00548	0.121273	0.12676	
0.0234	6.40622×10^{-10}	1133.8	73.46	0.02246	0.00550	0.12124	0.12674	0,2448
0.02345	6.41991×10^{-10}	1133.6	73.45	0.0225	0.00551	0.121208	0.12672	
0.0235	6.43360×10^{-10}	1133.5	73.44	0.02255	0.00552	0.121175	0.1267	
0.02355	6.44728×10^{-10}	1133.3	73.44	0.0226	0.00553	0.121143	0.12667	
0.0236	6.46097×10^{-10}	1133.2	73.43	0.02265	0.00554	0.12111	0.12665	
0.02365	6.47466×10^{-10}	1133.0	73.43	0.0227	0.00556	0.121078	0.12663	
0.0237	6.48835×10^{-10}	1132.9	73.42	0.02274	0.00557	0.121045	0.12661	
0.02375	6.50204×10^{-10}	1132.7	73.41	0.02279	0.00558	0.121013	0.12659	0,2449
0.0238	6.51573×10^{-10}	1132.6	73.41	0.02284	0.00559	0.12098	0.12657	
0.02385	6.52941×10^{-10}	1132.4	73.4	0.02289	0.00560	0.120948	0.12655	
0.0239	6.54310×10^{-10}	1132.3	73.4	0.02293	0.00561	0.120916	0.12653	
0.02395	6.55679×10^{-10}	1132.1	73.39	0.02298	0.00563	0.120884	0.12651	
0.024	6.57048×10^{-10}	1132.0	73.39	0.02303	0.00564	0.120851	0.12649	
0.02405	6.58417×10^{-10}	1131.8	73.38	0.02308	0.00565	0.120819	0.12647	
0.0241	6.59786×10^{-10}	1131.7	73.37	0.02313	0.00566	0.120787	0.12645	
0.02415	6.61155×10^{-10}	1131.5	73.37	0.02317	0.00567	0.120755	0.12643	0,2451
...	...	...	...	...	...	...	...	...